CYCle: Choosing Your Collaborators Wisely to Enhance Collaborative Fairness in Decentralized Learning

Anonymous authors
Paper under double-blind review

Abstract

Collaborative learning (CL) enables multiple participants to jointly train machine learning (ML) models on decentralized data sources without raw data sharing. While the primary goal of CL is to maximize the expected accuracy gain for each participant, it is also important to ensure that the gains are **fairly** distributed. Specifically, no client should be negatively impacted by the collaboration, and the individual gains must ideally be commensurate with the contributions. Most existing CL algorithms require central coordination and focus on the gain maximization objective while ignoring collaborative fairness. In this work, we first show that the existing measure of collaborative fairness based on the correlation between accuracy values without and with collaboration has drawbacks because it does not account for negative collaboration gain. We argue that maximizing mean collaboration gain (MCG) while simultaneously minimizing the collaboration gain spread (CGS) is a fairer alternative. Next, we propose the CYCle protocol that enables individual participants in a private decentralized learning (PDL) framework to achieve this objective through a novel reputation scoring method based on gradient alignment between the local cross-entropy and distillation losses. We further extend the CYCle protocol to operate on top of gossip-based decentralized algorithms such as Gossip-SGD. For the simple mean estimation problem with two participants, we also theoretically show that CYCle performs better than standard FedAvg, especially when there is large statistical heterogeneity. Experiments on the CIFAR-10, CIFAR-100, and Fed-ISIC2019 datasets empirically demonstrate the effectiveness of the CYCle protocol to ensure positive and fair collaboration gain for all participants, even in cases where the data distributions of participants are highly skewed.

1 Introduction

Collaborative learning (CL) refers to a framework where several entities can work together by pooling their resources to achieve a common machine learning (ML) objective without sharing raw data. This approach offers particular advantages in domains like healthcare and finance that require access to extensive datasets, which can be difficult to acquire for any single entity due to the costs involved or privacy regulations such as HIPAA (Centers for Medicare & Medicaid Services, 1996) and GDPR (European Parliament & Council of the European Union, 2016; Albrecht, 2016). Federated learning (FL) (McMahan et al., 2017) is a specific case of CL that enables multiple entities to collectively train a shared model by sharing their respective model parameters or gradients with a central server for aggregation. However, FL methods can lead to information leakage associated with sharing gradients/parameter updates with an untrusted third-party server that can potentially carry out reconstruction attacks (Zhu et al., 2019; Zhao et al., 2020). Furthermore, most CL algorithms assume that all participating agents are contributing equally to the learning process. When this assumption is violated, there is little incentive for collaboration because the gains are not distributed fairly. To avoid these pitfalls, a fully decentralized learning algorithm that fairly rewards the contributions of individual participants is required.

Recent works have attempted to tackle the challenge of *collaborative fairness* (CF) in FL settings. Shapley value (SV) (Shapley et al., 1953) is often used to estimate marginal utility of participants in FL. However, computing the SV involves high computation and communication costs. To mitigate this problem, variants of

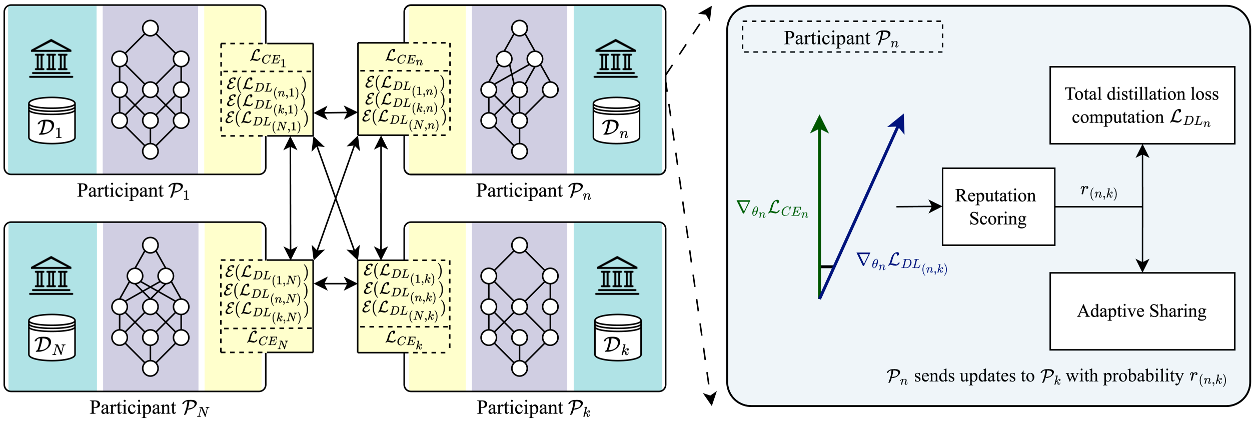
$\mathcal{L}_{CE_1}$
$\mathcal{E}(\mathcal{L}_{DL_{(n,1)}})$
$\mathcal{E}(\mathcal{L}_{DL_{(k,1)}})$
$\mathcal{E}(\mathcal{L}_{DL_{(N,1)}})$
$\mathcal{D}_1$
Participant $\mathcal{P}_1$
$\mathcal{L}_{CE_n}$
$\mathcal{E}(\mathcal{L}_{DL_{(1,n)}})$
$\mathcal{E}(\mathcal{L}_{DL_{(k,n)}})$
$\mathcal{E}(\mathcal{L}_{DL_{(N,n)}})$
$\mathcal{D}_n$
Participant $\mathcal{P}_n$
$\mathcal{E}(\mathcal{L}_{DL_{(1,N)}})$
$\mathcal{E}(\mathcal{L}_{DL_{(n,N)}})$
$\mathcal{E}(\mathcal{L}_{DL_{(k,N)}})$
$\mathcal{L}_{CE_N}$
$\mathcal{D}_N$
Participant $\mathcal{P}_N$
$\mathcal{E}(\mathcal{L}_{DL_{(1,k)}})$
$\mathcal{E}(\mathcal{L}_{DL_{(n,k)}})$
$\mathcal{E}(\mathcal{L}_{DL_{(N,k)}})$
$\mathcal{L}_{CE_k}$
$\mathcal{D}_k$
Participant $\mathcal{P}_k$
Participant $\mathcal{P}_n$
$\nabla_{\theta_n}\mathcal{L}_{CE_n}$
$\nabla_{\theta_n}\mathcal{L}_{DL_{(n,k)}}$
Reputation Scoring
$r_{(n,k)}$
Total distillation loss computation $\mathcal{L}_{DL_n}$
Adaptive Sharing
$\mathcal{P}_n$ sends updates to $\mathcal{P}_k$ with probability $r_{(n,k)}$

Figure 1: Illustration of the proposed Choose Your Collaborators Wisely (CYCle) protocol for Private Decentralized Learning (PDL).

SV have been proposed in Wang et al. (2020); Kumar et al. (2022); Xu et al. (2021); Tastan et al. (2024). But these methods only focus on FL with a central server. Existing private decentralized learning (PDL) algorithms such as CaPriDe learning (Tastan & Nandakumar, 2023), CaPC (Choquette-Choo et al., 2021), and Cronus (Chang et al., 2019) emphasize on confidentiality, privacy and utility, while ignoring collaborative fairness.

In this work, we aim to bridge this significant gap by designing the CYCle protocol for knowledge sharing in the PDL setting. We focus on three goals - maximizing the mean accuracy gain across all participants, ensuring that no participant suffers performance degradation due to collaboration, and the accuracy gains are evenly distributed. To achieve these goals, we make the following contributions:

- We analyze the *collaborative fairness metric* based on correlation coefficient between the contributions of participants and their respective final accuracies, and show that it fails in cases where the collaboration gain is negative.
- We introduce the *CYCle protocol* that regulates knowledge transfer among participants in a PDL framework based on their reputations to achieve better collaborative fairness. The proposed *reputation scoring* scheme uses gradient alignment between cross-entropy and distillation losses to accurately assess relative contributions made by collaborators in PDL.
- We extend the CYCle protocol to operate seamlessly on top of gossip-based decentralized algorithms such as Gossip-SGD, enabling fair collaboration.
- We theoretically study the CYCle protocol in the context of mean estimation between two participants and show that it outperforms FedAvg in the presence of data heterogeneity.

2 Related Work and Background

Several challenges associated with CL have been addressed recently, including privacy (Dwork et al., 2014; Choquette-Choo et al., 2021; Chang et al., 2019; Tastan & Nandakumar, 2023; Kairouz et al., 2021; Erlingsson et al., 2020; McMahan et al., 2018), confidentiality (Tastan & Nandakumar, 2023; Choquette-Choo et al., 2021; Chang et al., 2019), communication efficiency (McMahan et al., 2017), robustness (Lakshminarayanan et al., 2017; Athalye et al., 2018; Bagdasaryan et al., 2020), and fairness (Xu et al., 2021; Zhou et al., 2021; Lyu et al., 2020). Most existing works focus only on FL algorithms with central orchestration such as FedAvg (McMahan et al., 2017). Due to the potential harm caused by gradient leakage in FL (Zhao et al., 2020; Zhu et al., 2019), which can result in the disclosure of sensitive user data, there is a growing interest in decentralized learning algorithms that do not require centralized orchestration. Focus has been mainly on ensuring confidentiality, privacy, and utility in decentralized learning (Tastan & Nandakumar, 2023; Choquette-Choo et al., 2021; Chang et al., 2019).

To achieve collaborative fairness in CL, it is critical to evaluate marginal contributions of participants (Jia et al., 2019; Xu et al., 2021; Shi et al., 2022; Jiang et al., 2023; Tastan et al., 2024). The main reason to have a robust data valuation technique is the heterogeneous nature of data distribution across clients, meaning that some clients may contribute more useful data than others. In vanilla FL, all participants receive the same global model irrespective of their contributions, which can potentially discourage collaboration and increase resistance to practical adoption. While Shapley Value (SV) can be used for data valuation, SV computation is expensive and hard to employ (Shapley et al., 1953). In CGSV (Xu et al., 2021), cosine similarity between local and global parameter updates is used to approximate the SV. The same cosine similarity approach is used in RFFL (Xu & Lyu, 2021) for reputation scoring. Kumar et al. (2022) used logistic regression models as proxies for client data and utilized an ensemble of them to approximate the SVs.

2.1 Preliminaries

Notations. Let $\tilde{\mathcal{M}}_\theta : \mathcal{X} \to \mathcal{Y}$ be a supervised classifier parameterized by θ, where $\mathcal{X} \subseteq \mathbb{R}^d$ and $\mathcal{Y} = \{1, 2, \cdots, M\}$ denote the input and label spaces, respectively, d is the input dimensionality, and M is the number of classes. Let $\mathcal{M}_\theta : \mathcal{X} \to \mathcal{Z}$ denote a mapping from the input to the logits space ($\mathcal{Z} \subset \mathbb{R}^M$) and σ_T be a softmax function (with temperature parameter T) that maps the logits into a probability distribution $\boldsymbol{p} = \sigma_T(\boldsymbol{z})$ over the M classes. The sample is eventually assigned to the class with the highest probability. Given an input sample $\boldsymbol{x} \in \mathcal{X}$ and its ground truth label $y \in \mathcal{Y}$, let $\mathcal{L}_{CE}$ denote the cross entropy (CE) loss based on the prediction $\sigma_T(\mathcal{M}_\theta(\boldsymbol{x}))$ and y. We denote $\mathcal{L}_{DL_{(i,j)}}$ as the pairwise distillation loss between two models $\mathcal{M}_{\theta_i}$ and $\mathcal{M}_{\theta_j}$. For example, the distillation loss (DL) could be computed as KL divergence between $\sigma_T(\mathcal{M}_{\theta_i}(\boldsymbol{x}))$ and $\sigma_T(\mathcal{M}_{\theta_j}(\boldsymbol{x}))$. Note that other types of distillation losses (Gou et al., 2021) can also be used in lieu of KL divergence.

Decentralized Learning. Let N be the number of collaborating participants and $\mathcal{N} = \{1, 2, ..., N\}$. We assume that each participant $\mathcal{P}_n, n \in \mathcal{N}$ has its own local training dataset $\mathcal{D}_n$ and a hold-out validation set $\tilde{\mathcal{D}}_n$. Based on the local training set, each participant can learn a local ML model $\mathcal{M}_{\theta_n}$ by minimizing the local cross entropy loss $\mathcal{L}_{CE_n}$. The validation accuracy of this standalone local model $\mathcal{M}_{\theta_n}$ on $\tilde{\mathcal{D}}_n$ is denoted as $\mathcal{B}_n$. The goal in a typical FL algorithm is to build a single global model $\mathcal{M}_{\theta_*}$ that has a better accuracy than the standalone accuracy of all the local models. In contrast, the goal of each participant in decentralized learning is to obtain a better local model $\mathcal{M}_{\theta_n^*}$, which has a higher local validation accuracy $\mathcal{A}_n$ after collaboration. In other words, each participant $\mathcal{P}_n$ aims to maximize its *collaborative gain* (CG), which is defined as $\mathcal{G}_n = (\mathcal{A}_n - \mathcal{B}_n)$. This is typically achieved by minimizing the following objective:

$$\mathcal{L}_n = \mathcal{L}_{CE_n} + \lambda_n \mathcal{L}_{DL_n}, \tag{1}$$

where $\mathcal{L}_{DL_n}$ denotes the total distillation loss of $\mathcal{P}_n$ and $\lambda_n > 0$ is a hyperparameter that controls the relative importance of the cross entropy and distillation losses. Note that the term DL in the above formulation is used generically (without restricting to any specific loss function) and it intuitively captures the differences between the local model of a participant and the models of all its collaborators. The total DL of $\mathcal{P}_n$ can in turn computed by aggregating the pairwise distillation losses as follows:

$$\mathcal{L}_{DL_n} = \textstyle\sum_{k \in \mathcal{N} \setminus \{n\}} \lambda_{(n,k)} \mathcal{L}_{DL_{(n,k)}}, \tag{2}$$

where $\mathcal{L}_{DL_{(n,k)}}$ is the pairwise DL between $\mathcal{P}_n$ and $\mathcal{P}_k$ and $\lambda_{(n,k)}$ are the weights assigned to the pairwise losses between different participants.

Private Decentralized Learning (PDL). In the PDL framework, the total DL is computed in a privacy-preserving way without leaking the local data of participants. For example, CaPC learning (Choquette-Choo et al., 2021) leverages secure multi-party computation, homomorphic encryption, and differential privacy (DP) to securely estimate $\mathcal{L}_{DL_n}$. However, CaPC learning requires a semi-trusted third-party privacy guardian to privately aggregate local predictions and the pairwise distillation losses are not accessible. In contrast, CaPriDe learning (Tastan & Nandakumar, 2023) utilizes fully homomorphic encryption (FHE) to securely

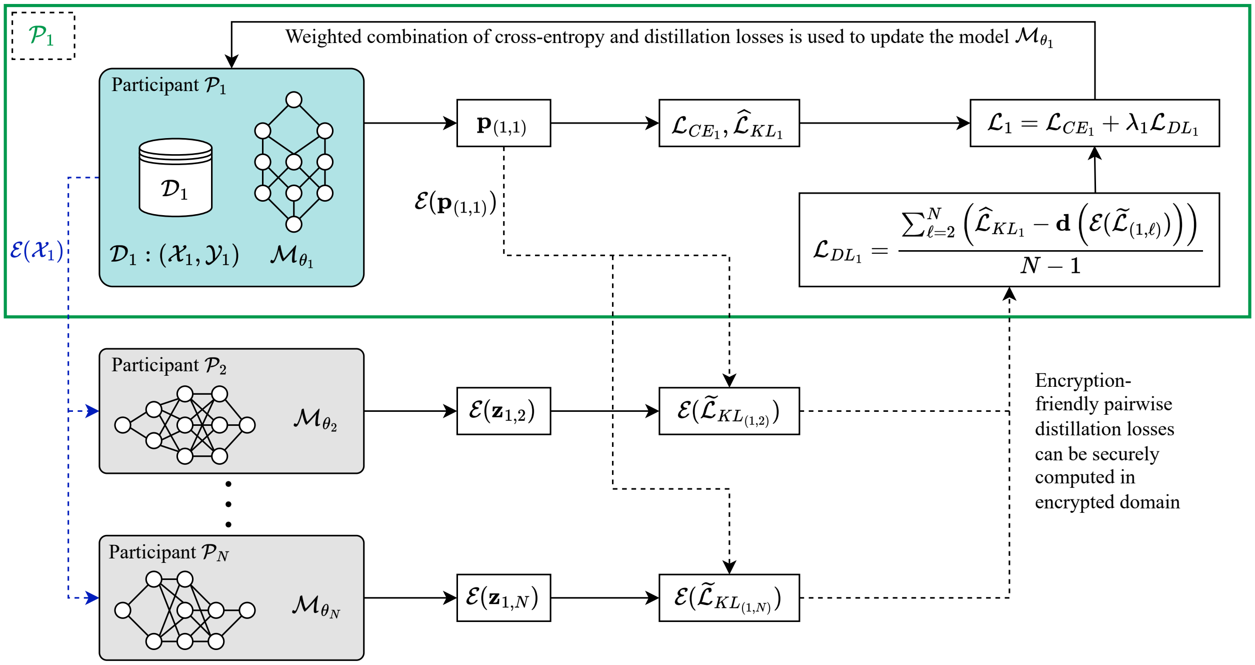
$\mathcal{P}_1$
Weighted combination of cross-entropy and distillation losses is used to update the model $\mathcal{M}_{\theta_1}$
Participant $\mathcal{P}_1$
$\mathcal{D}_1$
$\mathcal{D}_1 : (\mathcal{X}_1, \mathcal{Y}_1)$
$\mathcal{M}_{\theta_1}$
$\mathbf{p}_{(1,1)}$
$\mathcal{L}_{CE_1}, \widehat{\mathcal{L}}_{KL_1}$
$\mathcal{L}_1 = \mathcal{L}_{CE_1} + \lambda_1 \mathcal{L}_{DL_1}$
$\mathcal{E}(\mathbf{p}_{(1,1)})$
$\mathcal{L}_{DL_1} = \frac{\sum_{\ell=2}^{N} \left(\widehat{\mathcal{L}}_{KL_1} - \mathbf{d}\left(\mathcal{E}(\widetilde{\mathcal{L}}_{(1,\ell)})\right)\right)}{N-1}$
$\mathcal{E}(\mathcal{X}_1)$
Participant $\mathcal{P}_2$
$\mathcal{M}_{\theta_2}$
$\mathcal{E}(\mathbf{z}_{1,2})$
$\mathcal{E}(\widetilde{\mathcal{L}}_{KL_{(1,2)}})$
Encryption-friendly pairwise distillation losses can be securely computed in encrypted domain
Participant $\mathcal{P}_N$
$\mathcal{M}_{\theta_N}$
$\mathcal{E}(\mathbf{z}_{1,N})$
$\mathcal{E}(\widetilde{\mathcal{L}}_{KL_{(1,N)}})$

Figure 2: Illustration of confidential and private decentralized (CaPriDe) learning framework for N participants, showing the learning process for only participant $\mathcal{P}_1$. Here, $\mathcal{D}_1 = (\mathcal{X}_1, \mathcal{Y}_1) = \{\boldsymbol{x}_{j,1}, y_{j,1}\}_{j=1}^{|\mathcal{D}_1|}$ is the local data of $\mathcal{P}_1$, $\mathcal{E}(\mathcal{X}_1)$ denotes the collection of encrypted unlabeled samples of $\mathcal{P}_1$, and $\boldsymbol{p}_{(1,l)}$ and $\boldsymbol{z}_{(1,l)}$ are the prediction probabilities and logits obtained by applying model $\mathcal{M}_{\theta_l}$ of participant $\mathcal{P}_l$ to $\mathcal{X}_1$. Black dashed line represents exchange of encrypted data between participants in each round, and blue dashed line denotes a single transfer at the beginning of the protocol. $\boldsymbol{d}$ is a decryption method. $\mathcal{L}_{CE}$ and $\mathcal{L}_{DL}$ represent the cross-entropy and distillation losses, respectively. In the context of our paper, $\mathcal{L}_{DL_{(1,k)}} := \widehat{\mathcal{L}}_{KL_1} - \boldsymbol{d}\left(\mathcal{E}\left(\widetilde{\mathcal{L}}_{KL_{(1,k)}}\right)\right)$.

compute an approximation of the pairwise DL losses. However, all existing PDL algorithms lack a mechanism to assess the contributions of different participants within the CL framework. Hence, $\lambda_{(n,k)}$ is usually set to $\frac{1}{(N-1)}$ and $\lambda_n = \lambda_0, \ \forall \ n \in \mathcal{N}$. λ_0 is typically determined through hyperparameter search. We refer to the above scenario as *vanilla PDL* (VPDL).

CaPriDe Learning. CaPriDe learning framework (Tastan & Nandakumar, 2023), as described above, uses knowledge distillation approach and homomorphic encryption to enable secure and private computations. Figure 2 illustrates how CaPriDe learning works. Let $\mathcal{E}(\mathcal{X}_n) = \{\mathcal{E}(\boldsymbol{x}_{j,n})\}_{j=1}^{|\mathcal{D}_n|}$ be the collection of encrypted input samples of participant $\mathcal{P}_n$. Here, the encryption is based on a FHE scheme with public key of $\mathcal{P}_n$. In CaPriDe learning, each party initiates the collaboration by publishing $\mathcal{E}(\mathcal{X}_n)$ to the other participants. Let $\boldsymbol{z}_{j,(n,k)}$ and $\boldsymbol{p}_{j,(n,k)}$ denote the logits vector and probability vector obtained when model $\mathcal{M}_{\theta_k}$ of $\mathcal{P}_k$ is applied on the input sample $\boldsymbol{x}_{j,n}$, i.e., the j^{th} training sample of $\mathcal{P}_n$. Assume that at round $(t+1), 0 \leq t < \tau$ of the collaboration, the current model of $\mathcal{P}_n$ is $\mathcal{M}_{\theta_n^t}$. Then, $\mathcal{P}_n$ performs one forward pass on its own training set $\mathcal{D}_n$ to obtain the predictions $\{\boldsymbol{p}_{j,(n,n)}\}_{j=1}^{|\mathcal{D}_n|}$. To enable knowledge transfer between participants, CaPriDe learning makes use of the knowledge distillation (KD) approach (Hinton et al., 2015), where a student model learns to mimic the predictions of a teacher model. In CaPriDe learning, there is no designated teacher model, and mutual KD between multiple peer models is used for knowledge transfer. Let $\mathcal{L}_{DL_{(n,k)}}$ denote the pairwise distillation loss between predictions of $\mathcal{P}_n$ and $\mathcal{P}_k$, which is defined as:

$$\mathcal{L}_{DL_{(n,k)}} = \sum_{j=1}^{|\mathcal{D}_n|} D_{DL}\left(\boldsymbol{p}_{j,(n,n)}, \boldsymbol{p}_{j,(n,k)}\right) \tag{3}$$

$$= \widehat{\mathcal{L}}_{KL_n} - \boldsymbol{d}\left(\mathcal{E}\left(\widetilde{\mathcal{L}}_{KL_{(n,k)}}\right)\right) \tag{4}$$

where $D_{DL}(\boldsymbol{p}_1, \boldsymbol{p}_2)$ denotes the mimic distance between two predictions $\boldsymbol{p}_1$ and $\boldsymbol{p}_2$ and

$$\widehat{\mathcal{L}}_{KL_n} = \sum_{j=1}^{|\mathcal{D}_n|} \left(\boldsymbol{p}_{j,(n,n)} \cdot \log \boldsymbol{p}_{j,(n,n)}\right), \tag{5}$$

$$\mathcal{E}\left(\widetilde{\mathcal{L}}_{KL_{(n,k)}}\right) = \sum_{j=1}^{|\mathcal{D}_n|} \mathcal{E}\left(\boldsymbol{p}_{j,(n,n)}\right) \cdot \frac{\mathcal{E}\left(\boldsymbol{z}_{j,(n,k)}\right)}{T}, \tag{6}$$

where T is a temperature parameter and $\widetilde{\mathcal{L}}_{KL_{(n,k)}}$ is encryption-friendly, approximate KL divergence as per CaPriDe learning (Tastan & Nandakumar, 2023).

3 Towards a Better Fairness Metric

In (Lyu et al., 2020; Xu & Lyu, 2021), collaborative fairness (CF) is defined as follows:

Definition 1 (Collaborative Fairness)**.** In a federated system, a high-contribution participant should be rewarded with a better performing local model than a low-contribution participant. Mathematically, fairness can be quantified by the correlation coefficient between the contributions of participants and their respective final model accuracies.

In the above CF Definition 1, the contribution of a participant is typically evaluated based on its standalone local accuracy ($\mathcal{B}_n$). Thus, the CF metric attempts to ensure that participants with higher standalone accuracy receive a model with higher final accuracy ($\mathcal{A}_n$) compared to that received by other participants. However, the problem with this approach can be illustrated using a simple example. Consider two participants $\mathcal{P}_1$ and $\mathcal{P}_2$ with standalone accuracy of 60% and 80%, respectively. Suppose that after collaboration, $\mathcal{P}_1$ ($\mathcal{P}_2$) receives a model with an accuracy of 70% (70.1%). In this scenario, the system is considered perfectly fair (with a fairness measure of 1) according to the above CF definition, because $\mathcal{P}_2$ receives a model with higher accuracy compared to $\mathcal{P}_1$. However, it is obvious that only $\mathcal{P}_1$ benefits from this collaboration and achieves a CG of $\mathcal{G}_1 = 10\%$, whereas $\mathcal{P}_2$ gains nothing. Strictly speaking, $\mathcal{P}_1$ has a negative CG of $\mathcal{G}_2 = -9.9\%$, but it can always dump the collaboratively trained model and use its own standalone model to achieve zero CG. This scenario cannot be considered as fair, because the participant with the lower contribution benefits significantly without helping the participant with higher contribution.

The problem with CF quantification in Definition 1 is that it overlooks the scenario where the collaboration gain is negative. This is usually not the case in FL with iid settings, because all the participants have similar standalone accuracy and the accuracy of the collaboratively learned model is much higher than any of the individual standalone accuracies. However, in extreme non-iid settings (which is where collaborative fairness is most needed!), the problem of negative CG can be encountered often. Hence, there is a need for a better metric to quantify collaborative fairness.

One possible solution is to measure the rewards in terms of CG, instead of the final model accuracies. Consequently, fairness can be quantified by the correlation coefficient between the contributions of participants ($\mathcal{B}_n$) and their respective collaboration gains ($\mathcal{G}_n$). However, the drawback of this approach is that it is inherently much harder to improve the performance of the higher contribution participant who starts with a much higher standalone accuracy. Going back to the earlier example, if $\mathcal{P}_1$ improves from 60% to 70%, $\mathcal{P}_2$ has to improve its accuracy from 80% to more than 90% to achieve a fairness score of 1. While it is much easier to satisfy the first condition, it is hard to meet the second condition using any CL algorithm. Hence, the fairness metric based on the correlation between standalone accuracy and CG is likely to be negative for most cases, indicating poor fairness.

A better alternative is to minimize the probability that the CG is negative or zero, i.e., $P(\mathcal{G}_n \leq 0)$ should be small. Intuitively, this is possible only when the expected value (μ) of $\mathcal{G}_n$ is a large positive value and if the standard deviation (ν) of $\mathcal{G}_n$ is small. Mathematically, using the well-known Chebyshev single-tail inequality, we can show that $P(\mathcal{G}_n \leq 0)$ is bounded by $\frac{\nu^2}{\nu^2+\mu^2} = \frac{1}{(1+(\mu/\nu)^2)}$, provided $\mu > 0$. Thus, minimizing $P(\mathcal{G}_n \leq 0)$ requires maximizing μ and minimizing ν. Let the mean collaboration gain (MCG) and collaboration gain spread (CGS) be defined as the sample mean and standard deviation of CG across participants, i.e.,

$$\text{MCG} = \frac{1}{N}\sum_{n=1}^{N}\mathcal{G}_n, \qquad \text{CGS} = \sqrt{\frac{1}{(N-1)}\sum_{n=1}^{N}(\mathcal{G}_n - \text{MCG})^2}. \tag{7}$$

Hence, an ideal decentralized learning scheme should maximize MCG (achieve better utility), while at the same time minimize CGS (ensure that all participants benefit fairly). This minimizes the likelihood of a participant being negatively impacted by the collaboration (having negative CG).

4 Proposed CYCle Protocol

Assumptions and Scope. In this work, we restrict ourselves to the PDL framework presented in Eqs. 1 and 2. We also assume a cross-silo setting, where the number of participants is relatively small ($N < 10$) to ensure practical feasibility of PDL. Our method requires a PDL algorithm that can compute pairwise DL in a privacy- preserving way. While we employ CaPriDe learning (Tastan & Nandakumar, 2023) as the baseline method for PDL in this work, other alternatives can also be used. Complete description of the baseline PDL method and discussions about its convergence, communication efficiency, or privacy guarantees are beyond the scope of this work.

Rationale. To maximize its individual CG (and hence maximize MCG), each participant must intuitively give more importance to distillation losses corresponding to other reliable participants, while de-emphasizing distillation losses corresponding to unreliable participants. To minimize CGS, each participant must penalize other unreliable participants (who do not contribute to its own learning) by sharing less knowledge with them. To achieve both these goals, we need to solve the following two sub-problems: (i) **Reputation Scoring** (RS): How to efficiently evaluate the reliability/reputation $r_{(n,k)}$ of participant $\mathcal{P}_k$ in the context of collaborative learning of model $\mathcal{M}_{\theta_n^*}$ belonging to $\mathcal{P}_n$?, (ii) **Adaptive Sharing** (AS): How to regulate knowledge transfer among participants based on the reputation score to achieve collaborative fairness?.

Algorithm 1 CYCle $\left(t, k, \nabla_{\theta_n}\mathcal{L}_{CE_n}\right)$

```
Input: Momentum factor $\alpha$
$\phi \leftarrow$ Is Update Available from $\mathcal{P}_k$?
Reputation Scoring
if $\phi = 0$ then
    $\mathcal{L}_{DL_{(n,k)}} \leftarrow 0$
else
    $\mathcal{L}_{DL_{(n,k)}} \leftarrow$ Get DL from $\mathcal{P}_k$
    if $(t \mod R) = 0$ then
        $s \leftarrow \frac{1 - \cos(\nabla_{\theta_n}\mathcal{L}_{CE_n}, \nabla_{\theta_n}\mathcal{L}_{DL(n,k)})}{2}$
        $\tilde{r} \leftarrow h(s)$
        $r^t_{(n,k)} \leftarrow \alpha r^{t-1}_{(n,k)} + (1-\alpha)\tilde{r}$
    end if
end if
Adaptive Sharing
if $(t \mod R) = 0$ then
    Share predictions with $\mathcal{P}_k$
else
    $z \leftarrow \text{Uniform}([0,1])$
    if $z \leq r_{(k,n)}$ then
        Share predictions with $\mathcal{P}_k$
    end if
end if
return $\left(r^t_{(n,k)}, \mathcal{L}_{DL_{(n,k)}}\right)$
```

4.1 Reputation Scoring

Several reputation scoring methods have been proposed in the FL literature (Xu & Lyu, 2021; Zhang et al., 2021). These reputation scores are generally used by the FL server either for client selection or for weighted aggregation. In contrast to FL, where a global model is learned by a central server, each participant builds its own local model in PDL. Hence, it is not possible to compute a single reputation score for a PDL participant. Instead, each participant has its own local estimate of the reputation of other participants. Hence, the same participant may be assigned different reputation scores by its collaborators.

The proposed reputation scoring is based on the intuition that the gradient alignment between local CE loss and pairwise DL is a strong indicator of the utility of $\mathcal{P}_k$ to $\mathcal{P}_n$. For example, if the two gradients are completely misaligned (either because the data distributions of $\mathcal{P}_k$ and $\mathcal{P}_n$ do not have any overlap or because $\mathcal{P}_k$ is malicious), attempting to learn from $\mathcal{P}_k$ is likely to harm the learning of $\mathcal{P}_n$, rather than being beneficial. On the other hand, if there is perfect alignment, the two gradients reinforce each other and accelerate the model learning at $\mathcal{P}_n$. In fact, if KL divergence is used for pairwise DL computation, the gradients based on the local CE loss and pairwise DL will be closely aligned only when the predictions made by $\mathcal{P}_k$ on $\mathcal{P}_n$'s data closely match the ground-truth labels available with $\mathcal{P}_n$. This is because the CE loss measures the "distance" between $\sigma_T(\mathcal{M}_{\theta_n}(\boldsymbol{x}))$ and y, while the DL loss measures the "distance" between $\sigma_T(\mathcal{M}_{\theta_n}(\boldsymbol{x}))$ and $\sigma_T(\mathcal{M}_{\theta_k}(\boldsymbol{x}))$. These two losses will lead to aligned gradients only when $\sigma_T(\mathcal{M}_{\theta_k}(\boldsymbol{x}))$ is close to y. This justifies our choice of using gradient alignment between CE loss and pairwise DL as the basis for reputation scoring.

The reputation of a participant $\mathcal{P}_k$ from the perspective of $\mathcal{P}_n$ (denoted as $r_{(n,k)}$) is computed in two steps. First, the gradient (mis)alignment metric $s_{(n,k)}$ is computed as:

$$s_{(n,k)} = \frac{1 - \cos\left(\nabla_{\theta_n}\mathcal{L}_{CE_n}, \nabla_{\theta_n}\mathcal{L}_{DL_{(n,k)}}\right)}{2}, \tag{8}$$

where $\nabla_{\theta_n}\mathcal{L}_{CE_n}$ and $\nabla_{\theta_n}\mathcal{L}_{DL_{(n,k)}}$ are the gradients of cross entropy and distillation losses, respectively, with respect to the current parameters θ_n of the participant $\mathcal{P}_n$, $n \in \mathcal{N}$, and $k \in \mathcal{N}\backslash\{n\}$. Note that $s_{(n,k)} \to 0$ indicates better gradient alignment. We empirically observed that when the gradient alignment $s_{(n,k)}$ is below a threshold τ_{opt}, collaboration with $\mathcal{P}_k$ is mostly beneficial to $\mathcal{P}_n$. This is because as long as the predictions of $\mathcal{P}_k$ are closer to the ground-truth at $\mathcal{P}_n$, learning from $\mathcal{P}_k$ will help $\mathcal{P}_n$. In contrast, when $s_{(n,k)}$ is above a threshold τ_{max}, collaboration with $\mathcal{P}_k$ becomes harmful to $\mathcal{P}_n$. Based on these observations, we compute the reputation score by applying a soft clipping function to $s_{(n,k)}$. Specifically, the reputation score in the current round $\tilde{r}_{(n,k)} = h(s_{(n,k)})$, where h is defined as:

$$h(s) = \max\left(0, \min\left(1, \frac{s - \tau_{max}}{\tau_{opt} - \tau_{max}}\right)\right). \tag{9}$$

To minimize variations due to stochasticity, the reputation score is updated using a momentum factor, i.e., $r^t_{(n,k)} = \alpha r^{(t-1)}_{(n,k)} + (1-\alpha)\tilde{r}_{(n,k)}$, where $0 < \alpha < 1$ is the momentum hyperparameter and $r^t_{(n,k)}$ is the final reputation score in round t ($t > 0$). When $t = 0$, $r^t_{(n,k)} = \tilde{r}_{(n,k)}$. Henceforth, we drop the index t for convenience. A higher reputation score $r_{(n,k)}$ implies that updates from $\mathcal{P}_k$ are useful for model learning at $\mathcal{P}_n$. Hence, $\mathcal{P}_n$ can directly utilize $r_{(n,k)}$ to weight ($\lambda_{(n,k)}$) the pairwise distillation loss. While it is possible to perform reputation scoring and dynamically update the weights $\lambda_{(n,k)}$ after every collaboration round, it can also be performed periodically (after a fixed number of rounds) to minimize computational costs.

Algorithm 2 Private Decentralized Learning (PDL) based on Proposed CYCle Protocol

Input: Number of participants N, maximum communication rounds t_{max}, and learning rate η

Assumption: Each $\mathcal{P}_n$ has $\mathcal{D}_n = \{\boldsymbol{x}_{j,n}, y_{j,n}\}_{j=1}^{|\mathcal{D}_n|}$

```
$\mathcal{M}_{\theta_n^0} \leftarrow$ Local training at $\mathcal{P}_n$, $\forall\ n \in \mathcal{N}$
for each round $t = 0, 1, \cdots, t_{max}$ do
    for each participant $n \in \mathcal{N}$ do
        $\mathcal{L}_{CE_n} \leftarrow$ Compute cross-entropy loss of $\mathcal{P}_n$
        $\nabla_{\theta_n}\mathcal{L}_{CE_n} \leftarrow$ Compute the gradient of $\mathcal{L}_{CE_n}$
        for each participant $k \in \mathcal{N}\backslash\{n\}$ do
            $(r^t_{(n,k)}, \mathcal{L}_{DL_{(n,k)}}) \leftarrow$ CYCle$(t, k, \nabla\mathcal{L}_{CE_n})$
        end for
        $\lambda_{(n,k)} \leftarrow r^t_{(n,k)}$
        $\mathcal{L}_{DL_n} \leftarrow \sum_{k \in \mathcal{N}\backslash\{n\}} \lambda_{(n,k)} \cdot \mathcal{L}_{DL_{(n,k)}}$
        $\mathcal{L}_n \leftarrow \mathcal{L}_{CE_n} + \lambda_0 \cdot \mathcal{L}_{DL_n}$
        $\theta^t_n \leftarrow \theta^{t-1}_n - \eta\nabla_{\theta_n}\mathcal{L}_n$
    end for
end for
```

4.2 Adaptive Sharing

Once the reputation scores are computed, $\mathcal{P}_n$ can use $r_{(n,k)}$ to choose its collaborators wisely. Specifically, $\mathcal{P}_n$ can decide if it needs "*to share or not to share*" the distillation loss $\mathcal{L}_{DL_{(k,n)}}$ with $\mathcal{P}_k$. To be precise, $\mathcal{P}_n$ computes and sends $\mathcal{L}_{DL_{(k,n)}}$ to $\mathcal{P}_k$ with probability $r_{(n,k)}$. This adaptive sharing mechanism plays a key role in ensuring collaborative fairness. In order to receive updates from $\mathcal{P}_n$ in the current collaboration round, participant $\mathcal{P}_k$ needs to maintain a high reputation score with $\mathcal{P}_n$. This in turn requires sharing of updates that are useful for model learning at $\mathcal{P}_n$ in the previous round.

The above reputation-based adaptive sharing scheme has the following advantages: (1) It incentivizes $\mathcal{P}_k$ to share honest and useful updates with $\mathcal{P}_n$. Sharing noisy or malicious updates will hurt $\mathcal{P}_k$'s reputation score and hence, dampen $\mathcal{P}_k$'s ability to learn from $\mathcal{P}_n$. (2) If $\mathcal{P}_n$ finds that $\mathcal{P}_k$ has a low reputation score, it will send updates less frequently to $\mathcal{P}_k$, thereby saving valuable computational and communication resources. Note that in the PDL framework, privacy-preserving DL loss computation is often computationally expensive. However, there is one limitation in the proposed protocol. If $\mathcal{P}_n$ is malicious, it can deviate from the protocol and stop sending updates to $\mathcal{P}_k$ even though $r_{(n,k)}$ is high. While this can be addressed by penalizing participants (by reducing their reputation score) for not sharing updates, such an approach is not desirable because it will force participants to keep sharing updates even if they are not benefiting from the collaboration. Hence, we go for a compromise solution, where all the parties are forced to share updates after every R collaboration rounds and the reputation scores are re-calibrated based on these responses.

4.3 Mean Estimation as a Toy Example for CYCle Protocol

Consider a simple scenario involving two clients, $N = 2$, each aiming to estimate the mean of their data distributions (θ_1 and θ_2) by collaborating using the CYCle protocol. It can be shown that the probability of the estimate obtained through collaboration being better than a standalone estimate is lower bounded by $(1/8)\exp\left(-1/4\gamma^2\right)$, where γ is the variance of the standalone estimate (see Theorem A.1). More importantly, this bound is independent of the data heterogeneity, which contrasts with FedAvg. More details about this analysis are available in the supplementary material.

4.4 Extension to Gossip-SGD

We extend the CYCle protocol to operate on top of Gossip-SGD (Boyd et al., 2006; Koloskova et al., 2019) by modifying the collaborator selection mechanism through a dynamic, reputation-based mixing matrix. This matrix is periodically updated using gradient alignment scores and mapped via a softmax function parametrized by β to balance fairness and utility. At each communication round, collaborators are stochastically selected using Bernoulli sampling over this matrix, ensuring adaptive and meaningful knowledge exchange. Further implementation details and analysis are provided in Appendix C and D.3.

5 Experiments

Datasets. **CIFAR-10** (Krizhevsky et al., 2009) is a dataset consisting of 60000 images of size 32×32 pixels, categorized into 10 classes with 6000 images per class. It has 50000 training and 10000 test samples. **CIFAR-100** dataset (Krizhevsky et al., 2009) shares similarities with the CIFAR-10 dataset, but it consists of 100 classes with 600 samples per class. The training and test sets are divided in the same way as in CIFAR-10. CIFAR-100 dataset is used with data augmentation (random rotation (up to 15 degrees), random crop, and horizontal flip). **Fed-ISIC2019** (Ogier du Terrail et al., 2022) (from FLamby benchmark) is a multi-class dataset of dermoscopy images comprising of $23,247$ images with 8 different melanoma classes and high label imbalance (ranging from 49% to less than 1% for class 0 to 7). The dataset is designed for 6 clients based on the centers. Train/test split is: $(9930/2483), (3163/791), (2691/672), (1807/452)$, $(655/164), (351/88)$.

5.1 Experimental Setup

Baseline approaches. We consider several existing FL algorithms as baselines: vanilla FL based on FedAvg (FedAvg) (McMahan et al., 2017), FL based on cosine gradient Shapley value (CGSV) (Xu et al., 2021), collaborative fairness in FL (CFFL) (Lyu et al., 2020), and robust and fair FL (RFFL) (Xu & Lyu, 2021). The above methods are designed for FL with central orchestration. As mentioned earlier, the baseline VPDL method is based on CaPriDe learning (Tastan & Nandakumar, 2023). We also evaluate standalone (SA) accuracy, where each participant trains its ML model on its local dataset without any collaboration with others. Furthermore, we report the results for these baseline methods on CIFAR-10 and CIFAR-100.

Participant data splitting strategies. We implement three types of strategies to split the training dataset among the participants: (i) **homogeneous**, (ii) **heterogeneous**, and (iii) **imbalanced dataset**

sizes (denoted as 'imbalanced'). Homogeneous setting refers to the case where each participant gets an equal number of data points per class. In contrast, the heterogeneous method assigns a varying number of data points to each participant, based on a Dirichlet(δ) distribution. The parameter δ reflects the degree of non-IID characteristics within the dataset, where smaller values of δ leads to a more heterogeneous setting, while larger values tend towards an IID setting. To determine the specific allocation, we sample $p \sim Dir_N(\delta)$ and assign a fraction p_n of the total data samples to $\mathcal{P}_n$. We employ these settings for CIFAR-10 and CIFAR-100 with the following number of participants: $N = 2, 5, 10$. In all our experiments, we utilize all the training samples (e.g. all 50000 samples of CIFAR-10 and CIFAR-100). In the case of the imbalanced data distribution, we utilize a custom function that relies on parameters κ and m, where κ determines the proportion of data points received by each of the m chosen participants. The remaining $(N - m)$ participants then share the remaining data among themselves. We explore this setting with $N = 5$ participants and consider the following configurations: (i) imbalanced ($\kappa = 0.8$, $m = 1$), (ii) imbalanced ($\kappa = 0.35$, $m = 2$), and (iii) imbalanced ($\kappa = 0.6$, $m = 1$). For example, in the last case, one participant holds 60% of the data, while the remaining 4 participants get 10% of the data each.

Implementation details. We keep the same training hyperparameters for all experiments. Cross-entropy loss is used for local model training in all methods. The PDL algorithms (VPDL and CYCle) use Kullback-Leibler (KL) divergence based on predictions as the distillation loss. The optimizer is stochastic gradient descent (SGD) with momentum. The learning rate is initially set to 0.1 and is updated every 25 rounds using a scheduler with a learning rate decay of 0.1. For FL algorithms, we set the number of collaborating rounds to $t_{max} = 100$ and the local update epoch to 1. For the decentralized algorithms, we use 25 epochs of local training before collaboration, followed by 75 rounds of collaboration. The batch size is set to 128 for CIFAR-10 and CIFAR-100, and 32 for Fed-ISIC2019 dataset. Furthermore, $\alpha = 0.5$, $\lambda_0 = 50$, $\tau_{opt} = 0.25$ and $\tau_{max} = 0.75$. In the experiments involving Gossip-SGD, we set $\beta = 15$. We conduct our experiments on

Table 1: Performance comparison on CIFAR-10 dataset: Validation accuracy evaluated with $N = 5$ participants. The top section of the table presents the performance of our proposed framework compared to the FedAvg algorithm. The bottom part of the table compares collaboration gain and fairness of our proposed CYCle algorithm with existing works (rows 6-9). We employ MVA (↑), MCG (↑) and CGS (↓) as evaluation metrics.

Setting	**Homogeneous**			**Dirichlet (0.5)**			**Imbalanced (0.8, 1)**			**Imbalanced (0.35, 2)**			**Imbalanced (0.6, 1)**		
Metric	**MVA**	**MCG**	**CGS**	**MVA**	**MCG**	**CGS**	**MVA**	**MCG**	**CGS**	**MVA**	**MCG**	**CGS**	**MVA**	**MCG**	**CGS**
FedAvg	90.60	7.20	0.48	88.76	21.40	4.31	90.17	26.35	14.51	90.34	13.12	9.61	90.16	16.28	9.11
VPDL	84.98	1.58	0.71	74.27	6.91	2.31	67.18	3.36	3.58	78.71	1.49	4.01	75.43	1.55	2.45
CYCle	86.33	2.93	**0.32**	76.93	9.57	**2.07**	69.26	5.44	**2.56**	81.12	3.89	**2.65**	76.72	2.83	**1.38**
CFFL	62.65	2.21	0.87	49.04	2.49	2.35	58.66	3.48	4.39	65.08	9.99	9.95	65.20	14.35	9.79
RFFL	61.50	1.05	0.95	48.52	1.96	1.63	56.27	1.08	**2.45**	58.51	3.43	7.46	51.35	0.50	6.74
CGSV	63.27	2.83	0.94	54.45	7.90	3.40	55.96	0.78	9.32	61.99	6.91	11.34	61.34	10.49	11.23
CYCle	71.95	11.51	**0.58**	51.21	4.65	**1.11**	61.80	6.62	2.79	68.26	13.17	**7.12**	64.93	14.08	**6.22**

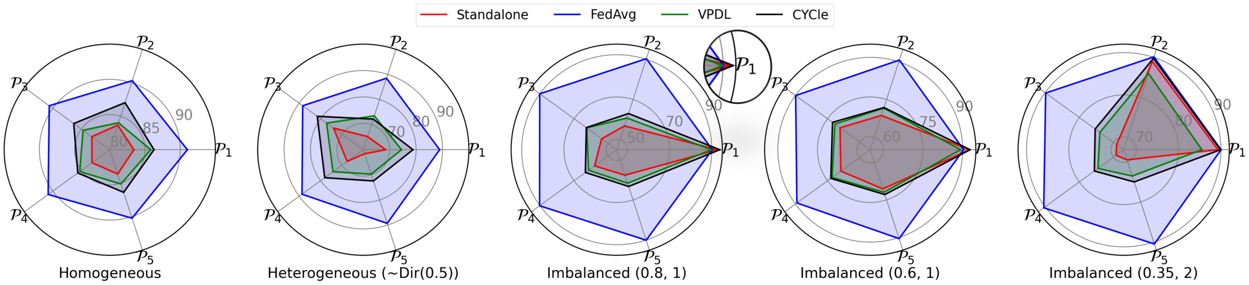

Homogeneous

Heterogeneous (~Dir(0.5))

Imbalanced (0.8, 1)

Imbalanced (0.6, 1)

Imbalanced (0.35, 2)

Figure 3: Per-participant performance comparison on CIFAR-10 dataset: Validation accuracy evaluated with $N = 5$ participants.

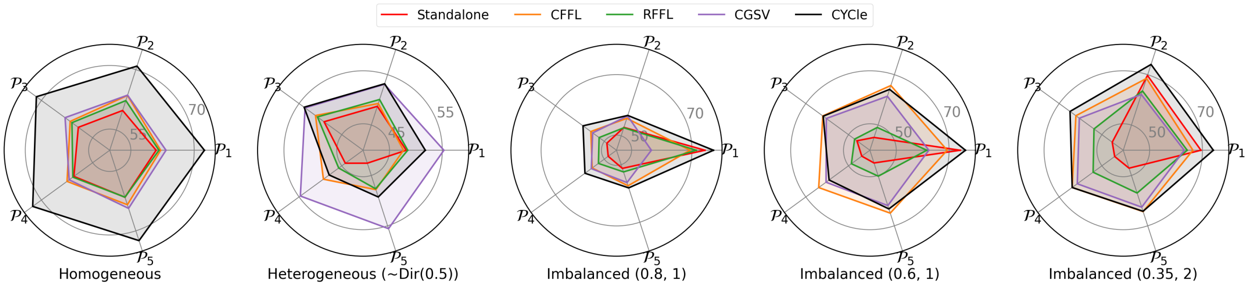

Figure 4: Per-participant performance comparison on CIFAR-10 dataset using custom CNN architecture from (Xu et al., 2021): Validation accuracy evaluated with $N = 5$ participants.

NVIDIA A100-PCIE-40GB GPUs on an internal cluster server, with each run utilizing a single GPU. The execution time for each run averages around 1.35 hours.

Evaluation metrics. We assess the accuracy of the trained models based on their mean validation accuracy (MVA) and mean collaboration gain (MCG) across all participants. To evaluate collaborative fairness, we use the collaboration gain spread (CGS). The reputation scores are reported in a matrix form to determine the relative contribution of each client.

5.2 Experimental Results

We start with benchmarking existing algorithms on the CIFAR-10 dataset. Table 1 summarizes the results for different splitting strategies involving $N = 5$ participants. Our key findings are:

(i) We assess the performance of three algorithms – FedAvg, VPDL, and CYCle – using the ResNet18 architecture. These results are shown in Figure 3 and the upper section of Table 1 (rows 3-5). FedAvg has better MCG compared to other methods due to its centralized FL approach, which involves aggregating and sharing full model parameters, resulting in good overall utility. However, when it comes to collaborative fairness, FedAvg falls short of being fair to participants who contribute a larger amount of data. In particular, the CYCle approach exhibits significantly lower CGS values compared to the FedAvg algorithm in the imbalanced settings. Additionally, our method consistently provides positive collaboration gain to all participants across varied settings. This is not the case for FedAvg or VPDL, which is evident in the outcomes for $\mathcal{P}_1$ in the imbalanced $(0.8, 1)$ and $(0.6, 1)$ settings.

(ii) For comparison with other fairness-aware FL algorithms, we utilize a custom CNN architecture used in Xu et al. (2021). This is necessary because CGSV works better on simpler architectures. The results are shown in Figure 4 and the bottom part of Table 1 (rows 6-9). Our method has better or comparable CG values when compared to CFFL, RFFL, and CGSV in most of the scenarios. In terms of fairness, we surpass other approaches by achieving the lowest CGS values in all but one scenario: imbalanced $(0.8, 1)$ setting, where it is on par with RFFL. Notably, CYCle consistently achieves positive gains for all participants, whereas other methods degrade performance for the most contributing participant (see Figure 4).

Next, we assess the performance of our approach on the CIFAR-10 and CIFAR-100 datasets with different number of participants ($N \in \{5, 10\}$) and data splitting scenarios (Table 2). In all the settings, we consistently achieve positive collaboration gain for all participants and the CYCle method consistently has lower CGS compared to VPDL, demonstrating improved fairness across participants. Additionally, we observe that when integrated with Gossip-SGD (DSGD), CYCle maintains this trend: while the baseline DSGD achieves high MCG values due to aggressive mixing, it often results in large CGS values, indicating significant disparity among participants. In contrast, CYCle significantly reduces CGS without compromising MCG, highlighting its ability to regulate knowledge flow more equitably in decentralized and peer-to-peer settings.

Table 2: Collaboration gain and spread (MCG, CGS) on CIFAR-10 and CIFAR-100 datasets and the given partition strategies for $N = \{5, 10\}$ using our proposed algorithm. DSGD refers to the Gossip-SGD algorithm.

Dataset		**CIFAR-10**						**CIFAR-100**					
N		**5**			**10**			**5**			**10**		
Split	**Method**	**MVA**	**MCG**	**CGS**	**MVA**	**MCG**	**CGS**	**MVA**	**MCG**	**CGS**	**MVA**	**MCG**	**CGS**
Homogeneous	VPDL	84.98	1.58	0.71	71.01	1.92	1.58	56.74	7.58	1.20	40.87	10.42	2.48
	CYCle	86.24	2.84	**0.37**	73.66	4.57	**0.71**	57.56	8.40	**0.69**	41.17	10.72	**1.15**
	DSGD	84.05	8.86	**0.16**	80.57	13.75	0.48	56.45	19.28	0.19	49.79	23.95	0.38
	CYCle	84.22	9.03	**0.16**	79.84	13.02	**0.30**	56.07	18.90	**0.12**	49.41	23.57	**0.23**
Dirichlet (0.5)	VPDL	74.27	6.91	2.31	50.64	1.24	2.24	46.36	10.51	2.59	27.70	3.41	2.80
	CYCle	76.93	9.57	**2.13**	53.82	4.42	**1.98**	47.98	12.13	**0.68**	28.47	4.18	**1.07**
	DSGD	81.83	22.98	3.54	77.16	28.26	4.92	50.16	21.74	2.84	44.38	24.12	2.11
	CYCle	81.14	22.30	**2.60**	75.82	26.92	**3.71**	49.61	21.19	**0.95**	43.91	23.65	**1.16**
Dirichlet (2.0)	VPDL	81.26	3.38	3.72	69.36	5.51	5.00	56.31	12.43	2.31	39.34	9.71	3.16
	CYCle	83.13	5.25	**2.42**	72.33	8.48	**4.83**	57.61	13.73	**2.14**	39.93	10.30	**1.97**
	DSGD	83.66	12.64	0.97	79.86	18.25	2.29	55.53	21.19	0.97	50.21	25.89	0.61
	CYCle	83.48	12.45	**0.68**	79.64	18.03	**1.87**	56.36	22.01	**0.89**	50.59	26.27	**0.57**
Dirichlet (5.0)	VPDL	83.32	2.39	1.94	72.37	4.54	3.96	58.18	9.80	1.38	41.86	10.03	2.92
	CYCle	84.80	3.86	**1.15**	74.83	7.00	**3.72**	59.67	11.29	**1.08**	41.92	10.09	**1.38**
	DSGD	83.72	10.02	0.56	80.38	15.65	1.17	56.06	20.02	0.54	50.33	24.94	0.67
	CYCle	83.85	10.15	**0.33**	80.46	15.73	**0.77**	55.87	19.83	**0.48**	49.62	24.24	**0.43**

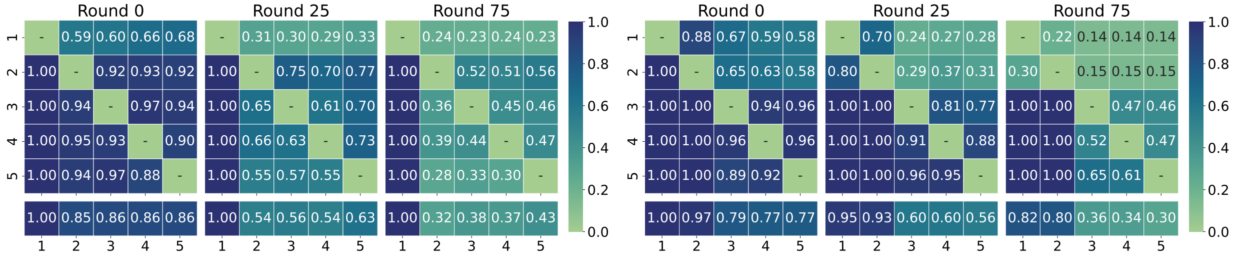

(a) Imbalanced (0.8, 1) setting

(b) Imbalanced (0.35, 2) setting

Figure 5: Heatmap visualization of reputation scores for imbalanced settings when $N = 5$.

Reputation scoring visualization. Figure 5 visualizes the computed reputation scores in three collaboration rounds: $t = 0, 25, 75$ using heatmap plots. In Figure 5a, where participants have imbalanced data (with $\mathcal{P}_1$ having 80% of the data), our method can already identify distinct patterns of each participant's data value from the beginning of the collaboration. The heatmap figure emphasizes that the higher is importance given to $\mathcal{P}_1$ by all the other participants. As the collaboration progresses, the reputation of $\mathcal{P}_1$ intensifies further, while the reputation scores of other participants decrease. Towards the end of the collaboration, the values converge to a state where participants with an equal amount of data receive equal reputation scores. A similar pattern can be observed in Figure 5b, where the first two participants possess larger amounts of data. While the first five rows of the heatmap figures depict the raw reputation scores calculated using Equation 9, the sixth row at the bottom represents the average reputation scores aggregated over all the rounds.

Free Rider Study. In this study involving $N = 5$ participants with homogeneous data splitting scenario, we simulate varying degrees of label flipping at participant $\mathcal{P}_5$. We tested the label flipping rates of 0.2, 0.5 and 1.0. From Figure 6, it is evident that the honest participants (participants $\mathcal{P}_1, \ldots, \mathcal{P}_4$) quickly discern the anomaly with $\mathcal{P}_5$, detecting it as a potential threat. Consequently, they assign a reputation score of 0.0 to $\mathcal{P}_5$, indicating a cessation of updates to this participant. On the other hand, $\mathcal{P}_5$ accurately recognized that the other participants were beneficial when the label flipping rate was at 0.2, but this positive assessment drops to zero for the case when the label space of $\mathcal{P}_5$ become completely different.

Table 3: Validation accuracies of participants ($\mathcal{P}_1$, ..., $\mathcal{P}_5$) with $\mathcal{P}_5$ having varying rates of label flipping. The last column refers to the average accuracy of honest participants ($\mathcal{P}_1$, ..., $\mathcal{P}_4$). The corresponding figure with reputation scores: Fig. 6.

Setting	$\mathcal{P}_1$	$\mathcal{P}_2$	$\mathcal{P}_3$	$\mathcal{P}_4$	$\mathcal{P}_5$	**avg**
Standalone ($\mathcal{B}_n$)	83.42	83.67	83.15	83.13	83.63	83.34
Flip rate = 0.0	86.12	87.03	86.33	85.62	86.10	86.28
Flip rate = 0.2	84.95	84.5	84.5	86.45	60.95	85.10
Flip rate = 0.5	84.25	84.65	84.65	83.25	55.80	84.20
Flip rate = 1.0	83.9	84.5	83.95	85.1	10.75	84.36

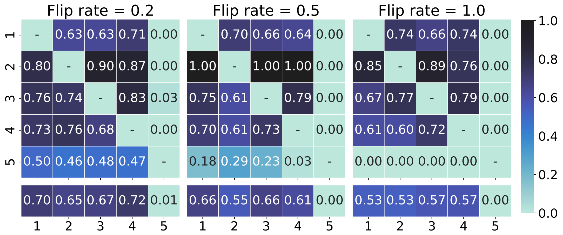

Figure 6: Heatmap visualization of reputation scores when the labels at one of the participants $\mathcal{P}_5$ get corrupted by label flipping. When the flip rate is large, the "malicious" client is quickly identified by the other participants.

Table 3, aligned with Figure 6, details the values of $\mathcal{B}_n$ and $\mathcal{A}_n$. It reveals that, in the presence of flipped labels, the collaboration gain declines, reflecting a loss from a participant that holds 20% of the data.

Trade-off between MCG and CGS. Figure 7 presents a plot depicting the MCG and CGS values for 10 different data-split scenarios, which are specified in Table 1 and Table 8. It must be emphasized that the outcomes of our CYCle approach fall predominantly towards the bottom-right corner of the plot, indicating higher MCG and lower CGS values. On average, CYCle achieves the highest MCG and lowest CGS across the 10 scenarios. While competing methods (CFFL, RFFL, and CGSV) may slightly perform better than CYCle in one metric, they perform significantly worse in the other.

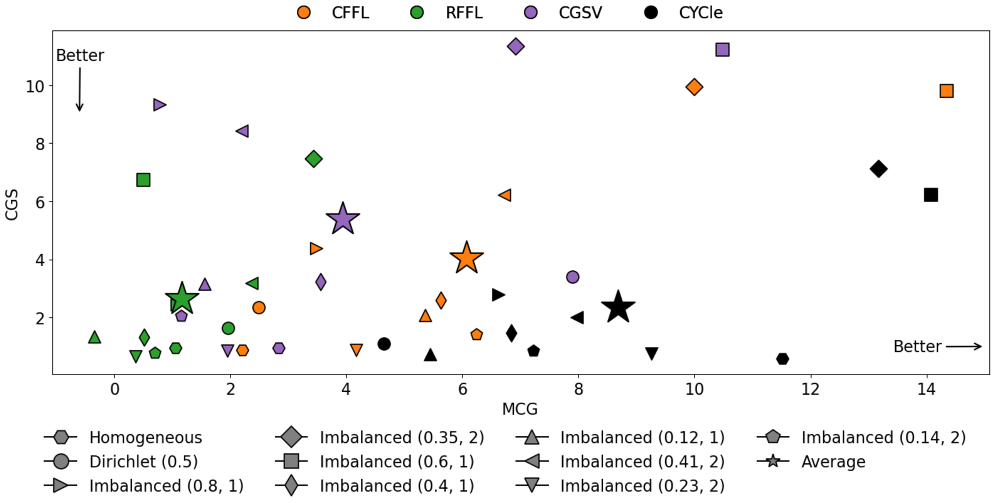

Figure 7: Plot of MCG and CGS values for 10 distinct data splits, ranging from homogeneous to a spectrum of imbalanced scenarios.

6 Conclusion

This paper proposed a novel reputation-based adaptive sharing algorithm to promote collaborative fairness, specifically tailored for decentralized learning scenarios. By leveraging gradient alignment, CYCle dynamically adjusts knowledge transfer based on participants' contributions, ensuring positive and equitable collaboration gains. We further extended the protocol to operate seamlessly over gossip-based decentralized learning algorithms. Through theoretical and empirical analyses, this work has illustrated the algorithm's superior capabilities in achieving collaborative fairness.

References

Jan Philipp Albrecht. How the gdpr will change the world. *Eur. Data Prot. L. Rev.*, 2:287, 2016.

Anish Athalye, Nicholas Carlini, and David Wagner. Obfuscated gradients give a false sense of security: Circumventing defenses to adversarial examples. In *International conference on machine learning*, pp. 274–283. PMLR, 2018.

Eugene Bagdasaryan, Andreas Veit, Yiqing Hua, Deborah Estrin, and Vitaly Shmatikov. How to backdoor federated learning. In *International Conference on Artificial Intelligence and Statistics*, pp. 2938–2948. PMLR, 2020.

Stephen Boyd, Arpita Ghosh, Balaji Prabhakar, and Devavrat Shah. Randomized gossip algorithms. *IEEE transactions on information theory*, 52(6):2508–2530, 2006.

Centers for Medicare & Medicaid Services. The Health Insurance Portability and Accountability Act of 1996 (HIPAA). Online at http://www.cms.hhs.gov/hipaa/, 1996.

Hongyan Chang, Virat Shejwalkar, Reza Shokri, and Amir Houmansadr. Cronus: Robust and heterogeneous collaborative learning with black-box knowledge transfer. *arXiv preprint arXiv:1912.11279*, 2019.

Yae Jee Cho, Divyansh Jhunjhunwala, Tian Li, Virginia Smith, and Gauri Joshi. To federate or not to federate: incentivizing client participation in federated learning. In *Workshop on Federated Learning: Recent Advances and New Challenges (in Conjunction with NeurIPS 2022)*, 2022.

Yae Jee Cho, Divyansh Jhunjhunwala, Tian Li, Virginia Smith, and Gauri Joshi. Maximizing global model appeal in federated learning. *Transactions on Machine Learning Research*, 2024. ISSN 2835-8856. URL `https://openreview.net/forum?id=8GI1SXqJBk`.

Christopher A. Choquette-Choo, Natalie Dullerud, Adam Dziedzic, Yunxiang Zhang, Somesh Jha, Nicolas Papernot, and Xiao Wang. CaPC Learning: Confidential and Private Collaborative Learning. In *International Conference on Learning Representations*, 2021. URL `https://openreview.net/forum?id=h2EbJ4_wMVq`.

Cynthia Dwork, Aaron Roth, et al. The algorithmic foundations of differential privacy. *Foundations and Trends® in Theoretical Computer Science*, 9(3–4):211–407, 2014.

Úlfar Erlingsson, Vitaly Feldman, Ilya Mironov, Ananth Raghunathan, Shuang Song, Kunal Talwar, and Abhradeep Thakurta. Encode, shuffle, analyze privacy revisited: Formalizations and empirical evaluation. *arXiv preprint arXiv:2001.03618*, 2020.

European Parliament and Council of the European Union. Regulation (EU) 2016/679 of the European Parliament and of the Council, The General Data Protection Regulation ("GDPR"), 2016. URL `https://data.europa.eu/eli/reg/2016/679/oj`.

Jianping Gou, Baosheng Yu, Stephen J Maybank, and Dacheng Tao. Knowledge distillation: A survey. *International Journal of Computer Vision*, 129:1789–1819, 2021.

Geoffrey Hinton, Oriol Vinyals, and Jeff Dean. Distilling the knowledge in a neural network, 2015. URL `https://arxiv.org/abs/1503.02531`.

Ruoxi Jia, David Dao, Boxin Wang, Frances Ann Hubis, Nick Hynes, Nezihe Merve Gürel, Bo Li, Ce Zhang, Dawn Song, and Costas J Spanos. Towards efficient data valuation based on the shapley value. In *The 22nd International Conference on Artificial Intelligence and Statistics*, pp. 1167–1176. PMLR, 2019.

Meirui Jiang, Holger R. Roth, Wenqi Li, Dong Yang, Can Zhao, Vishwesh Nath, Daguang Xu, Qi Dou, and Ziyue Xu. Fair federated medical image segmentation via client contribution estimation. In *Proceedings of the IEEE/CVF Conference on Computer Vision and Pattern Recognition (CVPR)*, pp. 16302–16311, June 2023.

Peter Kairouz, Ziyu Liu, and Thomas Steinke. The distributed discrete gaussian mechanism for federated learning with secure aggregation. In *International Conference on Machine Learning*, pp. 5201–5212. PMLR, 2021.

Anastasia Koloskova, Sebastian Stich, and Martin Jaggi. Decentralized stochastic optimization and gossip algorithms with compressed communication. In *International Conference on Machine Learning*, pp. 3478–3487. PMLR, 2019.

Anastasia Koloskova, Nicolas Loizou, Sadra Boreiri, Martin Jaggi, and Sebastian Stich. A unified theory of decentralized sgd with changing topology and local updates. In *International Conference on Machine Learning*, pp. 5381–5393. PMLR, 2020.

Alex Krizhevsky, Geoffrey Hinton, et al. Learning multiple layers of features from tiny images. *Toronto, ON, Canada*, 2009.

Sourav Kumar, A Lakshminarayanan, Ken Chang, Feri Guretno, Ivan Ho Mien, Jayashree Kalpathy-Cramer, Pavitra Krishnaswamy, and Praveer Singh. Towards more efficient data valuation in healthcare federated learning using ensembling. In *Distributed, Collaborative, and Federated Learning, and Affordable AI and Healthcare for Resource Diverse Global Health: Third MICCAI Workshop, DeCaF 2022, and Second MICCAI Workshop, FAIR 2022, Held in Conjunction with MICCAI 2022, Singapore, September 18 and 22, 2022, Proceedings*, pp. 119–129. Springer, 2022.

Balaji Lakshminarayanan, Alexander Pritzel, and Charles Blundell. Simple and scalable predictive uncertainty estimation using deep ensembles. *Advances in neural information processing systems*, 30, 2017.

Lingjuan Lyu, Xinyi Xu, Qian Wang, and Han Yu. Collaborative fairness in federated learning. *Federated Learning: Privacy and Incentive*, pp. 189–204, 2020.

Brendan McMahan, Eider Moore, Daniel Ramage, Seth Hampson, and Blaise Aguera y Arcas. Communication-efficient learning of deep networks from decentralized data. In *Artificial intelligence and statistics*, pp. 1273–1282. PMLR, 2017.

H. Brendan McMahan, Daniel Ramage, Kunal Talwar, and Li Zhang. Learning differentially private recurrent language models. In *International Conference on Learning Representations*, 2018. URL `https://openreview.net/forum?id=BJ0hF1Z0b`.

Jean Ogier du Terrail, Samy-Safwan Ayed, Edwige Cyffers, Felix Grimberg, Chaoyang He, Regis Loeb, Paul Mangold, Tanguy Marchand, Othmane Marfoq, Erum Mushtaq, Boris Muzellec, Constantin Philippenko, Santiago Silva, Maria Teleńczuk, Shadi Albarqouni, Salman Avestimehr, Aurélien Bellet, Aymeric Dieuleveut, Martin Jaggi, Sai Praneeth Karimireddy, Marco Lorenzi, Giovanni Neglia, Marc Tommasi, and Mathieu Andreux. Flamby: Datasets and benchmarks for cross-silo federated learning in realistic healthcare settings. In S. Koyejo, S. Mohamed, A. Agarwal, D. Belgrave, K. Cho, and A. Oh (eds.), *Advances in Neural Information Processing Systems*, volume 35, pp. 5315–5334. Curran Associates, Inc., 2022.

Lloyd S Shapley et al. A value for n-person games. *Princeton University Press Princeton*, 1953.

Zhuan Shi, Lan Zhang, Zhenyu Yao, Lingjuan Lyu, Cen Chen, Li Wang, Junhao Wang, and Xiang-Yang Li. FedFAIM: A model performance-based fair incentive mechanism for federated learning. *IEEE Transactions on Big Data*, 2022.

Nurbek Tastan and Karthik Nandakumar. CaPriDe Learning: Confidential and private decentralized learning based on encryption-friendly distillation loss. In *Proceedings of the IEEE/CVF Conference on Computer Vision and Pattern Recognition (CVPR)*, pp. 8084–8092, June 2023.

Nurbek Tastan, Samar Fares, Toluwani Aremu, Samuel Horváth, and Karthik Nandakumar. Redefining contributions: Shapley-driven federated learning. In Kate Larson (ed.), *Proceedings of the Thirty-Third International Joint Conference on Artificial Intelligence, IJCAI-24*, pp. 5009–5017. International Joint Conferences on Artificial Intelligence Organization, 8 2024. doi: 10.24963/ijcai.2024/554. URL `https://doi.org/10.24963/ijcai.2024/554`. Main Track.

Tianhao Wang, Johannes Rausch, Ce Zhang, Ruoxi Jia, and Dawn Song. A principled approach to data valuation for federated learning. *Federated Learning: Privacy and Incentive*, pp. 153–167, 2020.

Lin Xiao, Stephen Boyd, and Sanjay Lall. A scheme for robust distributed sensor fusion based on average consensus. In *IPSN 2005. Fourth International Symposium on Information Processing in Sensor Networks, 2005.*, pp. 63–70. IEEE, 2005.

Xinyi Xu and Lingjuan Lyu. A reputation mechanism is all you need: Collaborative fairness and adversarial robustness in federated learning. In *International Workshop on Federated Learning for User Privacy and Data Confidentiality in Conjunction with ICML 2021 (FL-ICML'21)*, 2021.

Xinyi Xu, Lingjuan Lyu, Xingjun Ma, Chenglin Miao, Chuan Sheng Foo, and Bryan Kian Hsiang Low. Gradient driven rewards to guarantee fairness in collaborative machine learning. *Advances in Neural Information Processing Systems*, 34:16104–16117, 2021.

Bicheng Ying, Kun Yuan, Yiming Chen, Hanbin Hu, Pan Pan, and Wotao Yin. Exponential graph is provably efficient for decentralized deep training. *Advances in Neural Information Processing Systems*, 34: 13975–13987, 2021.

Jingwen Zhang, Yuezhou Wu, and Rong Pan. Incentive mechanism for horizontal federated learning based on reputation and reverse auction. In *Proceedings of the Web Conference 2021*, pp. 947–956, 2021.

Bo Zhao, Konda Reddy Mopuri, and Hakan Bilen. idlg: Improved deep leakage from gradients. *arXiv preprint arXiv:2001.02610*, 2020.

Zirui Zhou, Lingyang Chu, Changxin Liu, Lanjun Wang, Jian Pei, and Yong Zhang. Towards fair federated learning. In *Proceedings of the 27th ACM SIGKDD Conference on Knowledge Discovery & Data Mining*, pp. 4100–4101, 2021.

Ligeng Zhu, Zhijian Liu, and Song Han. Deep leakage from gradients. *Advances in neural information processing systems*, 32, 2019.

Contents

1 Introduction 1

2 Related Work and Background 2
2.1 Preliminaries . . . 3

3 Towards a Better Fairness Metric 5

4 Proposed CYCle Protocol 6
4.1 Reputation Scoring . . . 6
4.2 Adaptive Sharing . . . 7
4.3 Mean Estimation as a Toy Example for CYCle Protocol . . . 8
4.4 Extension to Gossip-SGD . . . 8

5 Experiments 8
5.1 Experimental Setup . . . 8
5.2 Experimental Results . . . 10

6 Conclusion 12

A Mean Estimation under CYCle Protocol 17

B Numerical Experiments 20
B.1 Varying Degrees of Heterogeneity . . . 20
B.2 Imbalanced Data . . . 21

C Extension to Gossip-SGD 22
C.1 Gossip-SGD . . . 22
C.2 Integrating CYCle with Gossip-SGD . . . 24

D Additional Experimental Results 25
D.1 Reputation Score Visualization . . . 25
D.2 Remaining Results of Table 2 . . . 26
D.3 Fed-ISIC2019 experiments . . . 26
D.4 Experiments on CIFAR-100 . . . 28
D.5 Imbalanced Data Study . . . 29
D.6 Free Rider Study . . . 29
D.7 Hyperparameter Sensitivity . . . 30
D.8 Additional Results . . . 31

A Mean Estimation under CYCle Protocol

Standard FL. The vanilla FedAvg algorithm, a standard FL approach, does not ensure an optimal final model for all participants in a federated setting. Consider a simple scenario involving two clients, $N = 2$, each aiming to estimate the mean of their data distribution by minimizing the loss function $f_k(w) = (w - \theta_k)^2$. However, these clients can't compute the true mean directly due to having only N_k samples from their distributions, denoted $e_{k,j} \sim \mathcal{N}(\theta_k, \nu^2), \forall j \in [N_k]$. Consequently, they minimize the empirical loss function $F_k(w) = (w - \widehat{\theta}_k)^2 + (\widehat{\theta}_k - \theta_k)^2$, where $\widehat{\theta}_k = \frac{1}{N_k} \sum_{j=1}^{N_k} e_{k,j}$, leading to $\widehat{w}_k = \widehat{\theta}_k$ as the minimizer of $F_k(w)$.

Additionally, the following quantities are defined:

$$\gamma^2 \coloneqq \frac{\nu^2}{N}; \qquad \gamma_G^2 = \left(\frac{\theta_1 - \theta_2}{2}\right)^2 \tag{10}$$

Note that the distribution of the empirical means themselves are distributed normally, due to the linear additivity property of independent normal random variables. This setting is similar to (Cho et al., 2022; 2024), albeit with a few modifications.

$$\widehat{\theta}_1 \sim \mathcal{N}(\theta_1, \gamma^2); \qquad \widehat{\theta}_2 \sim \mathcal{N}(\theta_2, \gamma^2) \tag{11}$$

Lemma A.1. *(Cho et al., 2022) The probability (likelihood) that the model obtained from collaborative training outperforms the standalone training model is upper-bounded by* $2\exp\Big(-\frac{\gamma_G^2}{5\gamma^2}\Big)$ *in a standard FL framework.*

Proof. We analyze the probability that the global model obtained using FedAvg algorithm is superior to one trained independently (standalone). The model in the standard FL approach is defined as:

$$w = \frac{\widehat{\theta}_1 + \widehat{\theta}_2}{2} \tag{12}$$

Then, the **usefulness** of the federated model can be measured in the following way:

$$\begin{aligned}
&\mathbb{P}\Big((w - \theta_1)^2 \le (\widehat{\theta}_1 - \theta_1)^2\Big) \\
&\quad = \mathbb{P}\left(\left(\frac{\widehat{\theta}_1 + \widehat{\theta}_2}{2} - \theta_1\right)^2 \le (\widehat{\theta}_1 - \theta_1)^2\right) && (13) \\
&\quad = \mathbb{P}\left(\left(\frac{\widehat{\theta}_1 + \widehat{\theta}_2}{2} - \theta_1\right)^2 - (\widehat{\theta}_1 - \theta_1)^2 \le 0\right) && (14) \\
&\quad = \mathbb{P}\left(\left(\frac{\widehat{\theta}_2 - \widehat{\theta}_1}{2}\right)^2 + 2(\widehat{\theta}_1 - \theta_1)\left(\frac{\widehat{\theta}_2 - \widehat{\theta}_1}{2}\right) \le 0\right) && (15) \\
&\quad = \mathbb{P}\left(\left\{\left(\frac{\widehat{\theta}_2 - \widehat{\theta}_1}{2}\right)^2 + 2(\widehat{\theta}_1 - \theta_1)\left(\frac{\widehat{\theta}_2 - \widehat{\theta}_1}{2}\right) \le 0\right\} \cap \Big\{\widehat{\theta}_2 > \widehat{\theta}_1\Big\}\right) \\
&\qquad + \mathbb{P}\left(\left\{\left(\frac{\widehat{\theta}_2 - \widehat{\theta}_1}{2}\right)^2 + 2(\widehat{\theta}_1 - \theta_1)\left(\frac{\widehat{\theta}_2 - \widehat{\theta}_1}{2}\right) \le 0\right\} \cap \Big\{\widehat{\theta}_2 \le \widehat{\theta}_1\Big\}\right) && (16) \\
&\quad = \mathbb{P}\left(\left\{\left(\frac{\widehat{\theta}_2 - \widehat{\theta}_1}{2}\right) + 2(\widehat{\theta}_1 - \theta_1) \le 0\right\} \cap \Big\{\widehat{\theta}_2 > \widehat{\theta}_1\Big\}\right) \\
&\qquad + \mathbb{P}\left(\left\{\left(\frac{\widehat{\theta}_2 - \widehat{\theta}_1}{2}\right)^2 + 2(\widehat{\theta}_1 - \theta_1)\left(\frac{\widehat{\theta}_2 - \widehat{\theta}_1}{2}\right) \le 0\right\} \cap \Big\{\widehat{\theta}_2 \le \widehat{\theta}_1\Big\}\right) && (17)
\end{aligned}$$

$$\leq \mathbb{P}\left(\left(\frac{\widehat{\theta}_2-\widehat{\theta}_1}{2}\right)+2(\widehat{\theta}_1-\theta_1)\leq 0\right)+\mathbb{P}\left(\widehat{\theta}_2-\widehat{\theta}_1\leq 0\right) \tag{18}$$

$$= \mathbb{P}(Z_1\leq 0)+\mathbb{P}(Z_2\leq 0) \qquad \text{where } Z_1\sim\mathcal{N}\left(\gamma_G,\frac{5}{2}\gamma^2\right), Z_2\sim\mathcal{N}(2\gamma_G,2\gamma^2) \tag{19}$$

$$\leq \exp\left(-\frac{\gamma_G^2}{5\gamma^2}\right)+\exp\left(-\frac{\gamma_G^2}{\gamma^2}\right)\leq 2\exp\left(-\frac{\gamma_G^2}{5\gamma^2}\right) \tag{20}$$

where (14) uses $\mathbb{P}(A)=\mathbb{P}(A\cap B)+\mathbb{P}(A\cap B^C)$, (18) uses $\mathbb{P}(A\cap B)\leq\mathbb{P}(A)$, (19) uses the linear additivity property of independent normal random variables and (11), (20) uses a Chernoff bound.

$\square$

CYCle Algorithm. The CYCle algorithm uniquely incorporates the reputations of each client during the aggregation of their computed means. Considering the scenario from the perspective of Client 1, who possesses an estimate $\widehat{\theta}_1$ and receives $\widehat{\theta}_2$ from Client 2, the aggregation is expressed as:

$$w_1=\left(1-\frac{r_{1,2}}{2}\right)\widehat{\theta}_1+\frac{r_{1,2}}{2}\widehat{\theta}_2 \tag{21}$$

As CYCle operates on a decentralized principle, each client develops its final model based on individual reputations denoted by r. For example, for Client 2, the model is:

$$w_2=\left(1-\frac{r_{2,1}}{2}\right)\widehat{\theta}_2+\frac{r_{2,1}}{2}\widehat{\theta}_1 \tag{22}$$

Notably, w_1 and w_2 are not necessarily the same due to the distinct reputation scores. The following discussion will simplify the notation by dropping indices and focusing on the aggregation process from the perspective of Client 1.

Reputation Scoring. In the CYCle algorithm, each participant calculates the reputation of their collaborators by assessing the distance between their shared means, denoted as $d=\left(\frac{\widehat{\theta}_2-\widehat{\theta}_1}{2}\right)^2$. This distance is then used to determine their reputations as follows:

$$r=\begin{cases}1.0 & \text{if } d\leq 1\\ 2-d & \text{if } 1<d\leq 2\\ 0.0 & \text{if } d>2\end{cases} \tag{23}$$

Here, d represents the empirical heterogeneity parameter, referred to as $\widehat{\gamma}_G^2$. The rationale for the assigned values is based on the degree of heterogeneity (23):

- If $\widehat{\gamma}_G^2<1$, it indicates minimal heterogeneity, suggesting that participants can benefit significantly from collaboration.
- If $\widehat{\gamma}_G^2>2$, it signals substantial heterogeneity, advising participants to avoid collaboration.

Thus, the reputation scores are directly influenced by the empirical heterogeneity observed between the participants.

Cost Function. To evaluate the CYCle algorithm against the standard, centralized FL algorithm, we consider the empirical losses each participant ends up solving. In FedAvg, all clients achieve the common mean:

$$w=\frac{\widehat{\theta}_1+\widehat{\theta}_2}{2} \tag{24}$$

and the empirical loss for Client 1 is:

$$F_1(w) = F_1\left(\frac{\widehat{\theta}_1 + \widehat{\theta}_2}{2}\right) = \widehat{\gamma}_G^2 + (\widehat{\theta}_1 - \theta_1)^2 \tag{25}$$

This formulation shows that each client encounters non-reducible loss terms in the FedAvg algorithm. For the CYCle algorithm, the model aggregation is reputation-weighted:

$$w = \left(1 - \frac{r}{2}\right)\widehat{\theta}_1 + \frac{r}{2}\widehat{\theta}_2 \tag{26}$$

yielding the empirical loss:

$$F_1(w) = r^2\widehat{\gamma}_G^2 + (\widehat{\theta}_1 - \theta_1)^2 \tag{27}$$

In CYCle, the empirical heterogeneity parameter $\widehat{\gamma}_G^2$ is adjusted using the reputation scores r, allowing each client to potentially achieve a final model that is as good as or better than their standalone model. Conversely, in FedAvg, all clients share the same final model. As the heterogeneity between clients increases (γ_G^2), the efficacy (usefulness) of the global model significantly diminishes, as highlighted in Lemma A.1. This comparison illustrates the advantage of CYCle in managing heterogeneity among the participants to enhance individual outcomes.

Minimizing the CYCle Objective: Ensuring Positive Outcomes. Unlike standard FL where increasing true heterogeneity γ_G^2 drastically reduces the usefulness of the global model (as noted in Lemma A.1), CYCle modulates the aggregation phase using reputation scores which are derived from the empirical heterogeneity parameter $\widehat{\gamma}_G^2$ (23).

Theorem A.1. *The probability (likelihood) that the model obtained through collaboration (w) surpasses a standalone-trained model ($\widehat{\theta}$) is lower bounded by $\frac{1}{8}\exp\left(-\frac{1}{4\gamma^2}\right)$ in the CYCle algorithm.*

Proof. We assess the performance (usefulness) of the collaborative model for client i using:

$$\mathbb{P}\Big((w_i - \theta_i)^2 \leq (\widehat{\theta}_i - \theta_i)^2\Big) \tag{28}$$

This analysis includes both of the scenarios: (i) $\widehat{\theta}_1 = \widehat{\theta}_2$ which directly implies a probability of 1.0, and (ii) a significant difference between $\widehat{\theta}_1$ and $\widehat{\theta}_2$ ($\widehat{\gamma}_G^2 \gg 0$), leading to no collaboration, also resulting in a probability of 1.0. The CYCle algorithm is not interested in obtaining a final global model and each client is self-interested in minimizing their own objective functions.

Case 1: $\widehat{\gamma}_G^2 \leq 1$

$$\mathbb{P}\Big((w_1 - \theta_1)^2 \leq (\widehat{\theta}_1 - \theta_1)^2\Big) \tag{29}$$

$$= \mathbb{P}\Big((w_1 - \widehat{\theta}_1)^2 + 2(w_1 - \widehat{\theta}_1)(\widehat{\theta}_1 - \theta_1) \leq 0\Big) \tag{30}$$

$$= \mathbb{P}\left(\left(\frac{\widehat{\theta}_2 - \widehat{\theta}_1}{2}\right)^2 + 2\left(\frac{\widehat{\theta}_2 - \widehat{\theta}_1}{2}\right)(\widehat{\theta}_1 - \theta_1) \leq 0\right) \tag{31}$$

$$\begin{aligned} &= \mathbb{P}\left(\left\{\left(\frac{\widehat{\theta}_2 - \widehat{\theta}_1}{2}\right)^2 + 2\left(\frac{\widehat{\theta}_2 - \widehat{\theta}_1}{2}\right)(\widehat{\theta}_1 - \theta_1) \leq 0\right\} \cap \{\widehat{\theta}_2 > \widehat{\theta}_1\}\right) \\ &\quad + \mathbb{P}\left(\left\{\left(\frac{\widehat{\theta}_2 - \widehat{\theta}_1}{2}\right)^2 + 2\left(\frac{\widehat{\theta}_2 - \widehat{\theta}_1}{2}\right)(\widehat{\theta}_1 - \theta_1) \leq 0\right\} \cap \{\widehat{\theta}_2 \leq \widehat{\theta}_1\}\right) \end{aligned} \tag{32}$$

$$\geq \mathbb{P}\Big(\{1 + 2(\widehat{\theta}_1 - \theta_1) \leq 0\} \cap \{\widehat{\theta}_2 > \widehat{\theta}_1\}\Big) \tag{33}$$

$$= \mathbb{P}\Big(\{\widehat{\theta}_1 - \theta_1 \leq -\frac{1}{2}\} \cap \{\widehat{\theta}_2 > \widehat{\theta}_1\}\Big) \tag{34}$$

$$= \mathbb{P}(\widehat{\theta}_1 < \widehat{\theta}_2)\ \mathbb{P}\big(\widehat{\theta}_1 - \theta_1 \leq -\frac{1}{2} | \widehat{\theta}_1 < \widehat{\theta}_2\big) \tag{35}$$

$$\geq \mathbb{P}(\widehat{\theta}_1 < \widehat{\theta}_2)\ \mathbb{P}\big(\widehat{\theta}_1 - \theta_1 \leq -\frac{1}{2}\big) \tag{36}$$

$$= \mathbb{P}(\widehat{\theta}_1 < \widehat{\theta}_2)\ \mathbb{P}\big(Z > \frac{1}{2\gamma}\big) \quad \text{where } Z \sim \mathcal{N}(0,1) \tag{37}$$

$$\geq \frac{1}{8} \exp\Big(-\frac{1}{4\gamma^2}\Big) \tag{38}$$

where (31) uses the reputation score $r = 1$ when $\widehat{\gamma}_G^2 < 1$ (refer to (23)), (32) uses $\mathbb{P}(A) = \mathbb{P}(A \cap B) + \mathbb{P}(A \cap B^C)$, (33) uses the definition of $\widehat{\gamma}_G^2 \leq 1$ and the second part of expression can be dropped since $\widehat{\gamma}_G$ can take values from -1 to 0, it can be assigned zero probability, (36) uses $\mathbb{P}(A|B) \geq \mathbb{P}(A)$, (37) uses $\widehat{\theta}_1 - \theta_1 \sim \mathcal{N}(0, \gamma^2)$, (38) $\mathbb{P}(\widehat{\theta}_1 < \widehat{\theta}_2) \geq \frac{1}{2}$ and $\mathbb{P}(Z \geq x) \geq \frac{1}{4}\exp(-x^2)$ where $Z \sim \mathcal{N}(0,1)$. The similar bound can be found for the second client.

Case 2: $1 < \widehat{\gamma}_G^2 \leq 2$

In this case, we can follow the similar approach above and we get:

$$\mathbb{P}\Big((w_1 - \theta_1)^2 \leq (\widehat{\theta}_1 - \theta_1)^2\Big) \tag{39}$$

$$= \mathbb{P}\Big((w_1 - \widehat{\theta}_1)^2 + 2(w_1 - \widehat{\theta}_1)(\widehat{\theta}_1 - \theta_1) \leq 0\Big) \tag{40}$$

$$= \mathbb{P}\Big(\Big(\frac{r}{2}(\widehat{\theta}_2 - \widehat{\theta}_1)\Big)^2 + r(\widehat{\theta}_2 - \widehat{\theta}_1)(\widehat{\theta}_1 - \theta_1) \leq 0\Big) \tag{41}$$

$$= \mathbb{P}\Big(r\Big(\frac{\widehat{\theta}_2 - \widehat{\theta}_1}{2}\Big)^2 + 2\Big(\frac{\widehat{\theta}_2 - \widehat{\theta}_1}{2}\Big)(\widehat{\theta}_1 - \theta_1) \leq 0\Big) \tag{42}$$

$$\geq \mathbb{P}\Big(\big\{1 + 2(\widehat{\theta}_1 - \theta_1) \leq 0\big\} \cap \big\{\widehat{\theta}_2 > \widehat{\theta}_1\big\}\Big) \tag{43}$$

$$\geq \frac{1}{8} \exp\Big(-\frac{1}{4\gamma^2}\Big) \tag{44}$$

The reason behind getting the same bound as in Case 1 is that the expression in (42) is maximized when $r = (2 - \widehat{\gamma}_G^2) = 1$, which necessitates $\widehat{\gamma}_G \approx 1$, when $\widehat{\theta}_1 < \widehat{\theta}_2$.

Case 3: $\widehat{\gamma}_G^2 > 2$

$$\mathbb{P}\Big((w_1 - \theta_1)^2 \leq (\widehat{\theta}_1 - \theta_1)^2\Big) = \Big((\widehat{\theta}_1 - \theta_1)^2 \leq (\widehat{\theta}_1 - \theta_1)^2\Big) = 1 \tag{45}$$

where $w_1 = \Big(1 - \dfrac{r}{2}\Big)\widehat{\theta}_1 + \dfrac{r}{2}\widehat{\theta}_2 = \widehat{\theta}_1$, since $r = 0$ for $\widehat{\gamma}_G^2 > 2$ (Eqs. 26, 23).

As such, CYCle effectively adapts to various degrees of heterogeneity, ensuring that collaboration invariably enhances or matches the standalone training performance. This is quantitatively supported by a lower bound of $\dfrac{1}{8}\exp\Big(-\dfrac{1}{4\gamma^2}\Big)$, demonstrating robustness against heterogeneity effects.

□

B Numerical Experiments

B.1 Varying Degrees of Heterogeneity

For the first experiment, we adopt the scenario outlined in previous studies (Cho et al., 2022; 2024). For the simulation involving two clients, we define the true means of the clients as $\theta_1 = 0, \theta_2 = \gamma_G$ where $\gamma_G \in [0, 5]$. The empirical means, $\widehat{\theta}_1$ and $\widehat{\theta}_2$, are sampled from the distribution $\mathcal{N}(\theta_1, 1)$ and $\mathcal{N}(\theta_2, 1)$ respectively, with equal sample sizes ($N_1 = N_2 = N$). The average usefulness is calculated over 10000 runs.

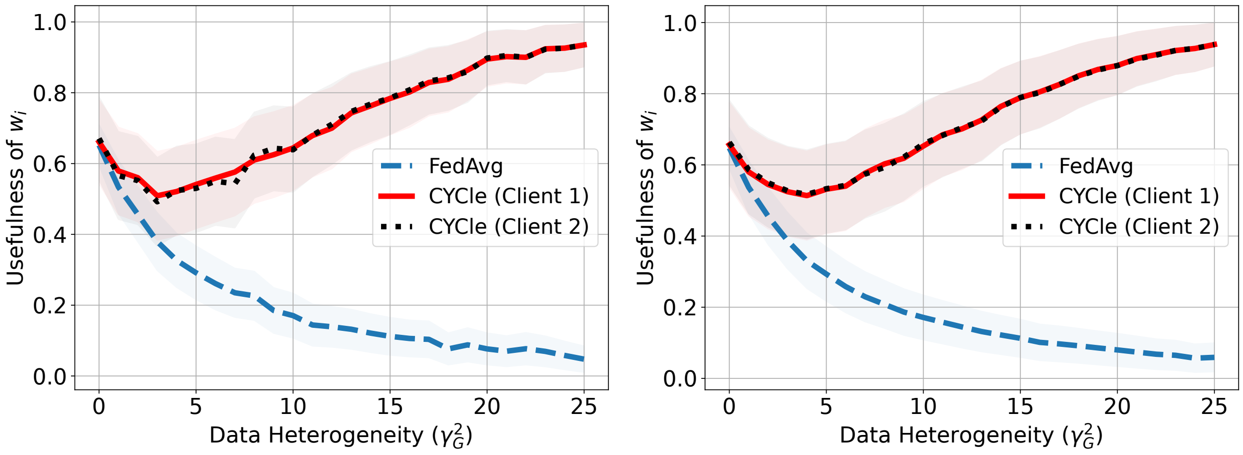

(a) Over 1000 runs

(b) Over 10000 runs

Figure 8: Numerical study on the usefulness of the model obtained after collaboration ($\mathbb{P}((w_i-\theta_i)^2 \leq (\widehat{\theta}_i-\theta_i)^2)$) in two client mean estimation. In FedAvg, a single global model is used, whereas in CYCle, each client computes their model (w_i) independently.

The results, depicted in Figure 8, highlight the differing impacts of heterogeneity on the final model's usefulness. Under the FedAvg protocol, as heterogeneity increases, the global model's usefulness drops drastically, potentially disadvantaging each client by diverging from their optimal solutions (empirical means). Conversely, the CYCle approach exhibits an increase in the usefulness of the resultant models (w_i) irrespective of the heterogeneity level. This indicates an effective mechanism within CYCle for clients to discern and select good collaborators based on the proximity of their updates. In scenarios of pronounced heterogeneity, resulting in low reputation scores, clients are incentivized to rely more heavily on their own updates, effectively mitigating collaboration when it proves detrimental.

B.2 Imbalanced Data

In this experiment, we consider a scenario where both clients share the same true mean $\theta_1 = \theta_2 = 0$, effectively setting the true heterogeneity parameter $\gamma_G^2 = 0$. Despite this, the clients differ in their number of

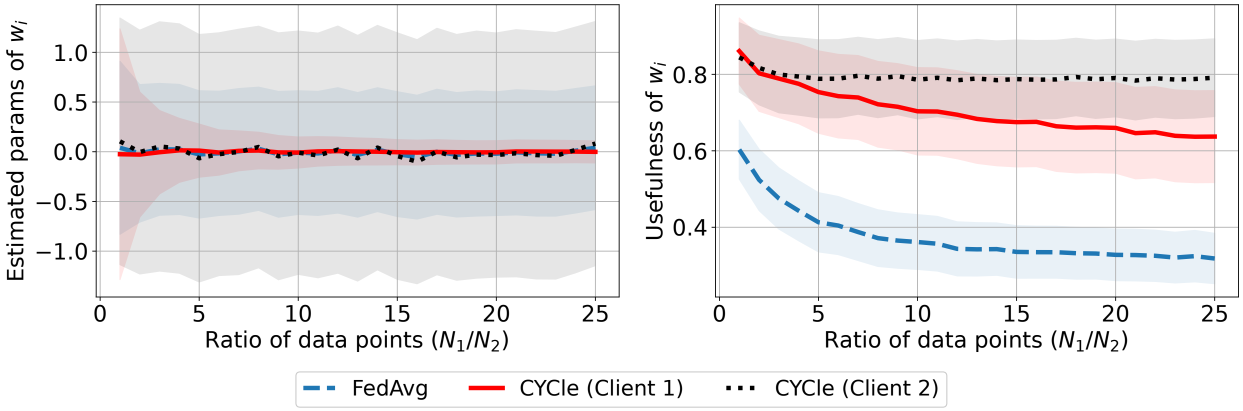

Figure 9: Numerical study on the impact of data imbalance on model usefulness ($\mathbb{P}((w_i-\theta_i)^2 \leq (\widehat{\theta}_i-\theta_i)^2)$) and the depiction of θ_i, σ_i estimates for $w_i \sim \mathcal{N}(\theta_i, \sigma_i^2)$ in two client mean estimation across varying degrees of data ratios.

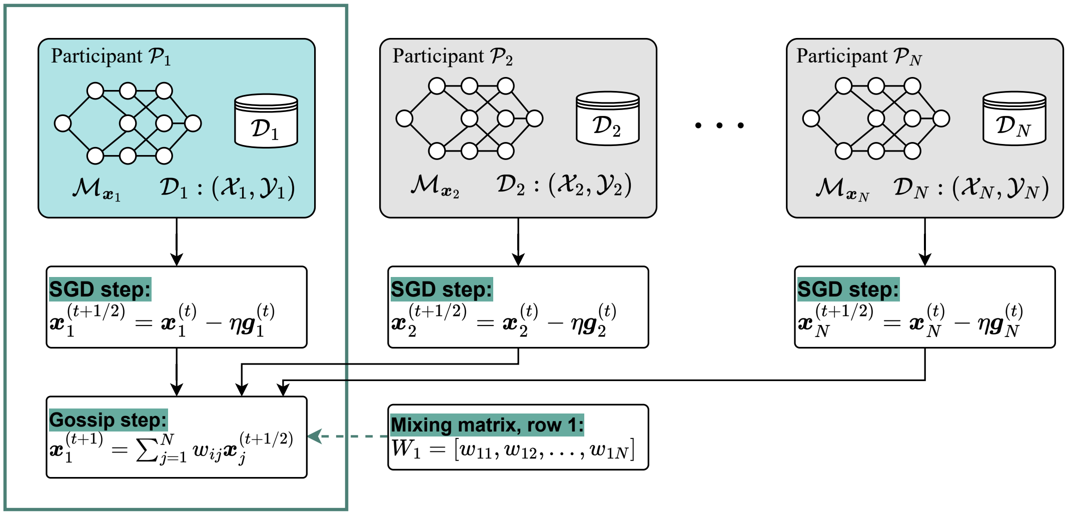
Participant $\mathcal{P}_1$
$\mathcal{D}_1$
$\mathcal{M}_{\boldsymbol{x}_1}$
$\mathcal{D}_1 : (\mathcal{X}_1, \mathcal{Y}_1)$
Participant $\mathcal{P}_2$
$\mathcal{D}_2$
$\mathcal{M}_{\boldsymbol{x}_2}$
$\mathcal{D}_2 : (\mathcal{X}_2, \mathcal{Y}_2)$
Participant $\mathcal{P}_N$
$\mathcal{D}_N$
$\mathcal{M}_{\boldsymbol{x}_N}$
$\mathcal{D}_N : (\mathcal{X}_N, \mathcal{Y}_N)$
SGD step: $\boldsymbol{x}_1^{(t+1/2)} = \boldsymbol{x}_1^{(t)} - \eta \boldsymbol{g}_1^{(t)}$
SGD step: $\boldsymbol{x}_2^{(t+1/2)} = \boldsymbol{x}_2^{(t)} - \eta \boldsymbol{g}_2^{(t)}$
SGD step: $\boldsymbol{x}_N^{(t+1/2)} = \boldsymbol{x}_N^{(t)} - \eta \boldsymbol{g}_N^{(t)}$
Gossip step: $\boldsymbol{x}_1^{(t+1)} = \sum_{j=1}^N w_{ij} \boldsymbol{x}_j^{(t+1/2)}$
Mixing matrix, row 1: $W_1 = [w_{11}, w_{12}, \dots, w_{1N}]$

Figure 10: Illustration of the Gossip-SGD algorithm for N participants, focusing on the learning process of participant $\mathcal{P}_1$. As depicted in the figure, each participant performs SGD updates locally, followed by a gossip step where they share and exchange with other participants.

samples, influencing their empirical means. Specifically, $\widehat{\theta}_1$ and $\widehat{\theta}_2$ are drawn from distributions $\mathcal{N}(0, \frac{\sigma^2}{N_1})$ and $\mathcal{N}(0, \frac{\sigma^2}{N_2})$, respectively, with σ^2 set to 5.

The results, presented in Figure 9, illustrate the differential impacts of collaboration based on sample size. Collaboration tends to benefit Client 2 more than Client 1, with Client 1 being the higher-contributing client in terms of data. The variance of Client 1 decreases as their data ratio increases, suggesting that Client 1 would benefit from limiting trust in Client 2's contributions under significant data imbalances. In contrast, the variance for Client 2 remains relatively the same regardless of the data ratio.

Figure 9 (right side) demonstrates the varying utilities of collaboration for each client. For Client 1, the usefulness of collaboration decreases as the data ratio becomes more skewed, whereas it remains constant for Client 2, implying that the collaboration is useful for Client 2. Notably, the FedAvg approach generally results in worse outcomes compared to both clients in the CYCle scenario, especially as imbalances in data contribution increase.

C Extension to Gossip-SGD

In this section, we extend our proposed algorithm, CYCle, to general decentralized optimization algorithms. Unlike the distillation-based approach described in Equations 1 and 2, which focuses on federated distillation settings, decentralized algorithms typically aim to solve the *average consensus problem*. This problem is formalized as:

$$\overline{\boldsymbol{x}} := \frac{1}{N} \sum_{i=1}^{N} \boldsymbol{x}_i, \tag{46}$$

where $\boldsymbol{x}_i \in \mathbb{R}^d$ are local vectors distributed across N nodes.

C.1 Gossip-SGD

Description of Gossip-SGD. Classic decentralized algorithms for solving the average consensus problem are often based on *gossip-based* algorithms (Xiao et al., 2005; Boyd et al., 2006; Koloskova et al., 2019; 2020; Ying et al., 2021) that generate sequences $\{\boldsymbol{x}_i^{(t)}\}_{t \geq 0}$ on every node $i \in [N]$ through iterative updates of the

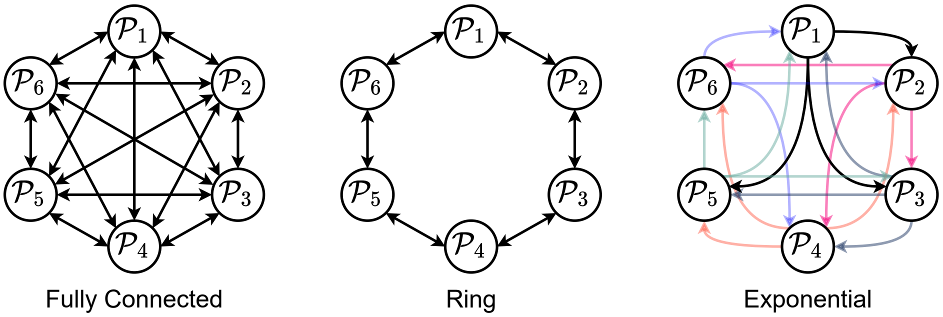

Figure 11: Different types of communication graphs/topologies: fully connected graph, ring graph and exponential graph.

form:

$$\boldsymbol{x}_i^{(t+1)} := \boldsymbol{x}_i^{(t)} + \eta \sum_{j=1}^{N} w_{ij} \Delta_{ij}^{(t)}, \tag{47}$$

where $\eta \in (0, 1]$ is a stepsize, $w_{ij} \in [0, 1]$ are the weights, and $\Delta_{ij}^{(t)} \in \mathbb{R}^d$ is the vector (e.g. gradients) sent from node j to node i at iteration t.

Communication occurs only if $w_{ij} > 0$, and no communication is needed when $w_{ij} = 0$. If the weights are symmetric ($w_{ij} = w_{ji}$), they define a communication graph $G = ([N], E)$ with edges $\{i, j\} \in E$ if $w_{ij} > 0$ and self-loops $\{i\} \in E$ for $i \in [N]$. The matrix $W \in \mathbb{R}^{N\times N}$, known as the *mixing* matrix or *gossip* matrix, specifies the connectivity of the network, with $(W)_{ij} = w_{ij}$.

The objective in decentralized optimization is to minimize the global function:

$$\min_{\boldsymbol{x}\in\mathbb{R}^{N\times d}} F(\boldsymbol{x}), \quad \text{where} \quad F(\boldsymbol{x}) = \sum_{i=1}^{N} f_i(\boldsymbol{x}_i), \tag{48}$$

where f_i represents the local objective at node i.

To solve the optimization problem in Equation 48, the Gossip-SGD algorithm alternates between the following two steps:

$$\boldsymbol{x}_i^{(t+1/2)} = \boldsymbol{x}_i^{(t)} - \eta \boldsymbol{g}_i^{(t)} \left(\mathbb{E}\left[\boldsymbol{g}_i^{(t)}\right] = \nabla f_i\left(\boldsymbol{x}_i^{(t)}\right)\right) \qquad \triangleright \ \textbf{SGD step} \tag{49}$$

$$\boldsymbol{x}_i^{(t+1)} = \sum_{j=1}^{N} w_{ij} \boldsymbol{x}_j^{(t+1/2)} \qquad \triangleright \ \textbf{Gossip step} \tag{50}$$

Combining both steps, the Gossip-SGD update in matrix form becomes:

$$\boldsymbol{x}^{(t+1)} = W\left(\boldsymbol{x}^{(t)} - \eta \boldsymbol{g}^{(t)}\right), \quad \text{where} \quad \boldsymbol{g}^{(t)} = \left(\boldsymbol{g}_1^{(t)}, \boldsymbol{g}_2^{(t)}, \dots, \boldsymbol{g}_N^{(t)}\right)^T \in \mathbb{R}^{N\times d}. \tag{51}$$

Communication topologies. Communication graphs play a critical role in decentralized learning, where these graphs define the communication topology, specifying which nodes (clients) can exchange model updates during training. Unlike standard federated learning (FL), where updates are aggregated by a central server, decentralized FL relies on peer-to-peer exchanges guided by the graph structure. Common topologies, as depicted in Figure 11, include

- *complete graphs*, where all nodes communicate directly;
- *ring graphs*, where nodes only communicate with their immediate neighbors; and

Algorithm 3 Gossip-SGD algorithm based on CYCle Protocol

```
Input: for each node $i \in [N]$ initialize $\boldsymbol{x}_i^{(0)} \in \mathbb{R}^d$, number of communication rounds $T$, stepsize $\eta$, and mixing matrix $W^{(0)}$
for round $t = 0, 1, \cdots, T$ do
    for each participant $i \in [N]$ in parallel do
        Compute $\boldsymbol{g}_i^{(t)} \leftarrow \nabla f_i\left(\boldsymbol{x}_i^{(t)}\right)$
        for each neighbor $j : \{i, j\} \in E$ and $(t \mod R = 0)$ do
            $s_{ij} \leftarrow \left(1 + \cos\left(\boldsymbol{g}_i^{(t)}, \boldsymbol{g}_j^{(t)}\right)\right)/2$
            $r_{ij} \leftarrow$ arbitrary mapping function$(s_{ij})$        ▷ softmax function
            $w_{ij}^{(t)} \leftarrow \alpha w_{ij} + (1-\alpha) r_{ij}$, with $\alpha = 0.5$
        end for
        $\boldsymbol{x}_i^{(t+1/2)} = \boldsymbol{x}_i^{(t)} - \eta \boldsymbol{g}_i^{(t)}$        ▷ stochastic gradient updates
    end for
    Construct $W$, $(W)_{ij} \leftarrow w_{ij}$
    Generate stochastic binary mask $S \leftarrow$ Bernoulli$(W)$
    Construct $\widetilde{W} \leftarrow W \odot S^T$ and normalize each row to sum up to 1
    $\boldsymbol{x}^{(t+1)} = \widetilde{W} \boldsymbol{x}^{t+1/2}$,    where $\boldsymbol{x}^{t+1/2} = \left(\boldsymbol{x}_1^{t+1/2}, \ldots, \boldsymbol{x}_N^{t+1/2}\right)$        ▷ gossip averaging
end for
```

- *exponential graphs*, which optimize connectivity while minimizing communication overhead.

The mixing matrix W is constructed using uniform weights based on the graph topology:

$$[W]_{ij} = \begin{cases} \dfrac{1}{|\mathcal{N}(i)| + 1}, & \text{if } (i,j) \in E \quad \text{or} \quad i = j, \\ 0, & \text{otherwise.} \end{cases} \tag{52}$$

where $|\mathcal{N}(i)|$ denotes the number of neighbors of node i.

In our work, we initialize the communication graph as a fully connected graph but incorporate two key mechanisms to make the topology dynamic: (i) reputation scoring and (ii) adaptive sharing (detailed in Section 4). These mechanisms allow the communication graph to evolve during training, enabling improved fairness. We detail the specifics in Section C.2.

C.2 Integrating CYCle with Gossip-SGD

Algorithm 3 illustrates how we extend the Gossip-SGD algorithm within the framework of our proposed CYCle protocol. The central modification involves the use of a dynamic mixing matrix, which is updated every R communication rounds. This update is guided by a reputation scoring mechanism based on gradient alignment and an adaptive sharing strategy. In this version of CYCle, we adopt a different mapping function than Equation 9, emphasizing the flexibility to use any mapping function, provided it preserves the probabilistic nature (i.e., maps values to the range [0, 1]). Specifically, we use a softmax function with a hyperparameter β. The parameter β controls the trade-off between utility and fairness: higher values of β penalize smaller cosine similarities, thereby promoting fairness, while lower values prioritize equity in updates, effectively emulating a fully-connected graph topology as a special case. During each communication round, we stochastically sample a binary matrix S from the mixing matrix W using Bernoulli sampling (or a coin toss). The resulting binary mask S determines the communication partners for that round, where updates are exchanged only between nodes corresponding to entries of 1.0 in S. This adaptive sharing mechanism enhances efficiency by facilitating productive collaborations and minimizing unproductive exchanges. Unlike PDL-based method, which conduct multiple communications within a single FL round and sample updates for distillation, our approach in Gossip-SGD performs the sampling over the communication rounds T. We evaluate this approach in Section D.3 on the Fed-ISIC2019 dataset. This dataset, being naturally partitioned and inherently non-IID, serves as a challenging and realistic benchmark for assessing federated learning algorithms.

D Additional Experimental Results

This section is organized in the following manner:

1. Heatmap visualizations of reputation scores for the remaining data splitting scenarios, which include homogeneous, Dirichlet (0.5), and imbalanced (0.6, 1) cases.
2. Remaining results of Table 2.
3. Details of the Fed-ISIC2019 data distribution and heatmap visualization of reputation scores for Fed-ISIC2019.
4. Experimental results on the CIFAR-100 dataset.
5. More analysis of the imbalanced data splitting scenario.
6. More analysis of the free rider scenario.
7. Trade-off between MCG and CGS.
8. Hyperparameter sensitivity.

D.1 Reputation Score Visualization

In Figure 12, we present the reputation scores calculated on the CIFAR-10 dataset for a group of five participants ($N = 5$). The figure illustrates the results at rounds $t = 0$, 25, 75, under different data partitioning schemes: (i) homogeneous, (ii) heterogeneous (Dirichlet ($\delta = 0.5$)), (iii) imbalanced ($\kappa = 0.6, m = 1$). In the homogeneous setting, participants have similar reputation scores that correlate with the sizes of the datasets they hold. Over time, these scores trend downwards as the cross-entropy loss gains prominence over the total distillation loss (Eq. 1). The heterogeneous and imbalanced (0.6, 1) scenarios exhibit a similar pattern, where the reputation scores align with the size of the data they possess. In the latter scenario, since $\mathcal{P}_1$ holds 60% of the data, its reputation remains consistent, prompting other participants to engage more actively in collaboration to receive updates from this major contributor.

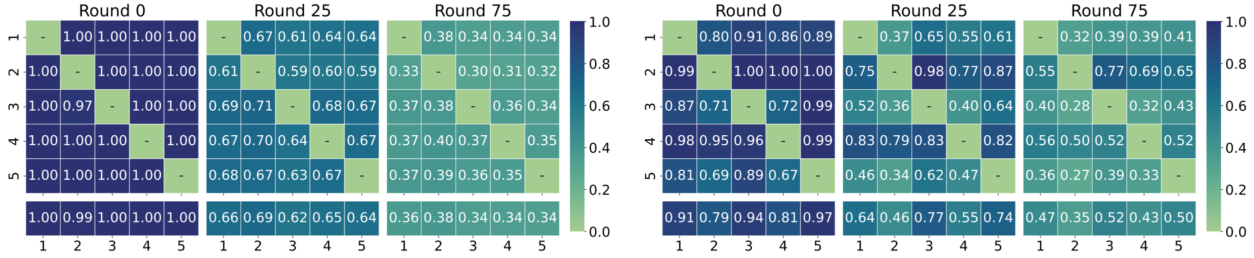

(a) Homogeneous setting

(b) Dirichlet (0.5) setting

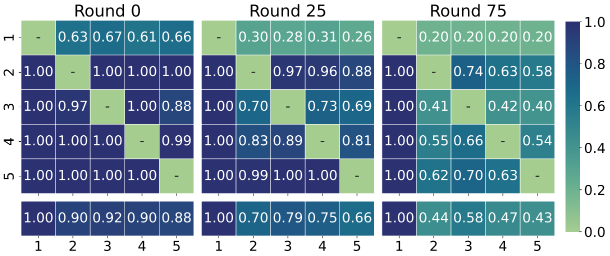

(c) Imbalanced (0.6, 1) setting

Figure 12: Heatmap visualization of reputation scores for the given number of participants $N = 5$ and data partition schemes: (a) Homogeneous, (b) Dirichlet (0.5) and (c) Imbalanced (0.6, 1).

It must be noted that even when dataset sizes are identical among participants, as seen in homogeneous ($\mathcal{P}_1$ to $\mathcal{P}_5$) and imbalanced (0.6, 1) ($\mathcal{P}_2$ to $\mathcal{P}_5$) data splitting scenarios, there may be stocahstic variations in data quality resulting in higher reputation scores for some participants compared to others. For instance, in Fig. 12c, $\mathcal{P}_3$ is assigned a marginally higher reputation score by the other participants, despite having an identical dataset size as $\mathcal{P}_2$, $\mathcal{P}_4$, and $\mathcal{P}_5$.

D.2 Remaining Results of Table 2

This section extends our analysis of collaboration gain and spread (MCG, CGS) for the CIFAR-10 and CIFAR-100 datasets using our proposed algorithm. While Table 2 focused on scenarios with $N \in \{5, 10\}$ participants, the additional results presented in Table 4 cover the scenario with $N = 2$ participants. This study provides further insight into the performance dynamics under a smaller number of participants and complements the study shown in Table 2.

Table 4: Collaboration gain and spread (MCG, CGS) on CIFAR-10 and CIFAR-100 datasets and the given partition strategies for $N = 2$ using our proposed algorithm. This table supplements Table 2, which covers $N = \{5, 10\}$.

Dataset		**CIFAR-10**			**CIFAR-100**			**Dataset**	**CIFAR-10**			**CIFAR-100**		
Split	**Method**	**MVA**	**MCG**	**CGS**	**MVA**	**MCG**	**CGS**	**Method**	**MVA**	**MCG**	**CGS**	**MVA**	**MCG**	**CGS**
Homogeneous	VPDL	91.99	0.41	0.08	71.52	4.87	0.55	DSGD	86.26	3.55	0.27	59.52	7.59	0.16
	CYCle	92.58	1.00	**0.01**	72.03	5.38	**0.22**	CYCle	86.36	3.64	**0.21**	59.53	7.61	**0.12**
Dirichlet (0.5)	VPDL	84.90	1.45	1.88	64.99	8.95	0.31	DSGD	84.03	16.92	12.51	55.95	10.73	8.13
	CYCle	88.82	5.37	**0.76**	66.37	10.33	**0.25**	CYCle	81.63	14.52	**9.24**	52.63	7.42	**5.11**
Dirichlet (2.0)	VPDL	89.93	0.09	0.22	70.57	5.52	0.66	DSGD	85.89	5.10	**1.51**	57.91	13.59	**0.71**
	CYCle	91.00	1.16	**0.15**	72.09	7.04	**0.18**	CYCle	86.53	5.73	**0.99**	57.81	13.50	**0.52**
Dirichlet (5.0)	VPDL	90.36	0.24	0.08	71.45	4.95	0.89	DSGD	85.92	3.77	0.91	58.93	9.83	0.33
	CYCle	91.29	1.17	**0.03**	72.12	5.62	**0.36**	CYCle	86.15	4.00	**0.58**	58.82	9.72	**0.11**

D.3 Fed-ISIC2019 experiments

Fed-ISIC2019: We evaluate our framework on the real-world non-IID Fed-ISIC2019 dataset. Note that for easy visualization, the participants in this experiment are sorted in the decreasing order of their dataset size. Fig. 13 illustrates the probability that each participant shared updates with their neighbors over $T = 100$ communication rounds. The reported values represent averages, for example, a value of 0.51 indicates that $\mathcal{P}_1$ shared updates with $\mathcal{P}_2$ during 51 out of 100 communication rounds. We observe that our framework captures distribution shift, as

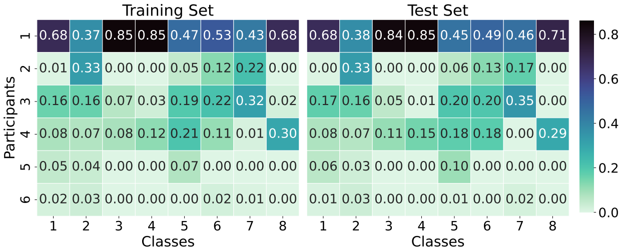

Figure 14: Fed-ISIC2019 data distribution.

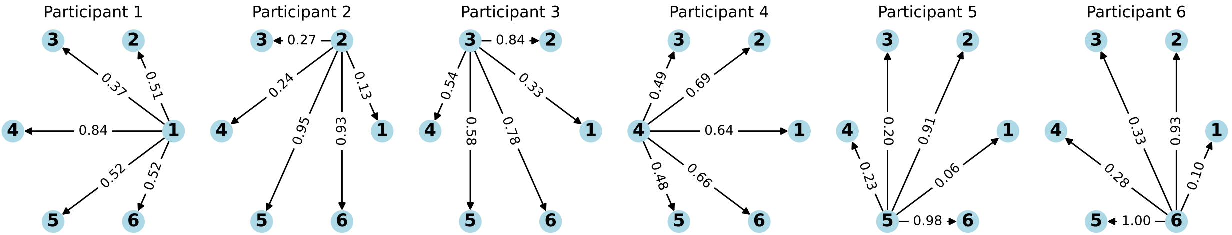

Figure 13: Illustration of communication graph over T communication rounds, representing the percentage of times each participant shared updates with its neighbors.

evidenced by the fact that the data held by the first client does not overlap with that of other clients (as shown in UMAP visualization in Figure 1f of Ogier du Terrail et al. (2022)).

Data Distribution. Figure 14 displays a heatmap plot illustrating the distribution of data by class among participants. In Figure 13, it is evident that despite $\mathcal{P}_1$ having the bulk of the data, it has a noticeable distribution shift compared to other participants. This indicates that other participants are not allocated certain classes due to the specific distribution settings employed in (Ogier du Terrail et al., 2022). It is noteworthy that initially, $\mathcal{P}_1$ assigns a lower reputation score to $\mathcal{P}_4$. However, over time, $\mathcal{P}_4$'s reputation improves, a change attributable to the exclusive knowledge of class 8 shared only by $\mathcal{P}_1$ and $\mathcal{P}_4$.

Experimental Results. Figure 15 illustrates the performance of the following methods: (i) standalone training, (ii) Gossip-SGD with a complete graph topology, (iii) Gossip-SGD with a ring topology, (iv) Gossip-SGD with an exponential graph topology, and (v) our proposed CYCle algorithm integrated with Gossip-SGD. The experiments span 100 communication rounds, and we report balanced accuracy as the primary metric due to the highly imbalanced nature of the classes. The results are derived from a global test set created by pooling the test sets of all participants to ensure a fair comparison.

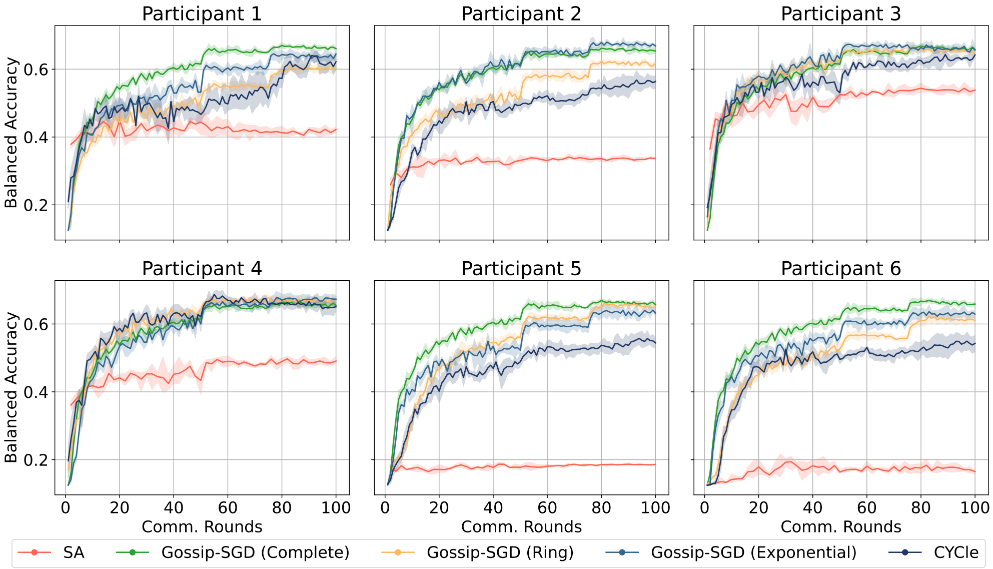

Figure 15: Per-participant performance plots on the Fed-ISIC2019 dataset comparing different methods: standalone training, Gossip-SGD with various topologies (fully connected, ring, exponential), and the proposed CYCle protocol. SA stands for standalone training.

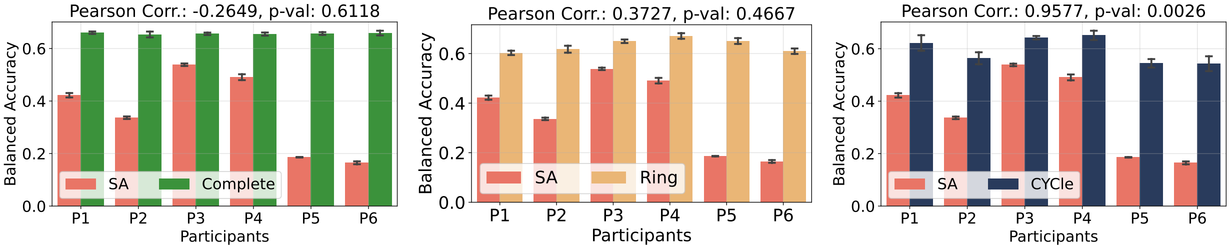

(a) Gossip-SGD with Complete Graph. (b) Gossip-SGD with Ring Graph. (c) CYCle with Dynamic Topology.

Figure 16: Per-participant accuracy and Pearson's correlation coefficient of the Gossip-SGD algorithm with fully connected and ring topologies, alongside the performance of our proposed CYCle algorithm. SA stands for standalone training.

Table 6: Per-participant performance comparison on CIFAR-100 dataset: Validation accuracy evaluated with $N = 5$ participants.

Partition	Number	SA	FedAvg	VPDL	CYCle
Homogeneous	1	48.85	70.25	57.05	56.10
	2	47.65	70.10	56.00	57.05
	3	48.45	69.55	57.30	57.10
	4	50.25	69.85	57.25	58.55
	5	50.60	70.35	56.10	59.00
Dirichlet (0.5)	1	39.40	69.20	48.15	50.35
	2	31.30	69.25	46.80	44.15
	3	38.00	67.80	47.00	49.80
	4	39.50	67.70	50.10	52.00
	5	31.05	67.60	39.75	43.60

Partition	Number	SA	FedAvg	VPDL	CYCle
Imbalanced (0.8, 1)	1	74.50	71.80	70.05	75.30
	2	20.80	73.45	27.40	29.85
	3	21.25	72.10	28.40	29.70
	4	22.25	72.10	28.50	30.20
	5	20.35	73.55	29.70	30.40
Imbalanced (0.35, 2)	1	61.45	70.00	62.10	67.15
	2	59.30	70.60	59.35	65.95
	3	29.65	70.55	40.15	39.80
	4	28.10	70.95	41.05	40.30
	5	32.05	69.55	39.75	41.95

Partition	Number	SA	FedAvg	VPDL	CYCle
Imbalanced (0.6, 1)	1	68.25	70.80	65.80	70.80
	2	29.90	70.90	39.30	39.00
	3	30.15	71.80	38.70	40.70
	4	28.50	71.35	39.45	38.05
	5	29.40	69.15	39.80	39.85

As shown in the plots, participants 5 and 6 struggle significantly, achieving performance below 20%. Interestingly, participants 3 and 4 achieve the best performance despite having smaller datasets compared to participants 1 and 2. Among the methods, Gossip-SGD with a complete graph topology achieves the highest overall performance. However, in terms of fairness (as shown in Figure 16a), it fails to provide equitable outcomes (Pearson's corr. coefficient of −0.2649), as all participants converge to a uniform final performance regardless of their contributions.

In contrast, our CYCle algorithm mitigates this issue by suppressing the collaboration gains of participants contributing less or providing low-quality updates. This results in a high correlation coefficient of 0.9577, with a small p-value of 0.0026, successfully rejecting the null hypothesis (that there is no correlation) at a significance level of 0.05 (see Figure 16c). These results highlight the efficacy of our approach in balancing both performance and fairness across participants. We also report the same plot for Gossip-SGD with a ring topology in Figure 16b, which fails to deliver fair outcomes for all participants. For the results on the MCG and CGS metrics, we refer the reader to Table 5.

Table 5: MCG and CGS values (Figure 15).

Method	MCG	CGS
Gossip-SGD (Complete)	30.26	15.64
Gossip-SGD (Ring)	27.72	14.80
Gossip-SGD (Exponential)	29.45	14.24
CYCle	23.79	**10.94**

D.4 Experiments on CIFAR-100

We perform the same experiment outlined in Table 1 and Figure 3 on CIFAR-100 dataset. Figure 17 and Table 6 depicts the performance of each participant within the $N = 5$ group across the various data partitioning strategies detailed in Section 5.1. Similar to the observations in Figure 3, in the imbalanced (0.8, 1) scenario,

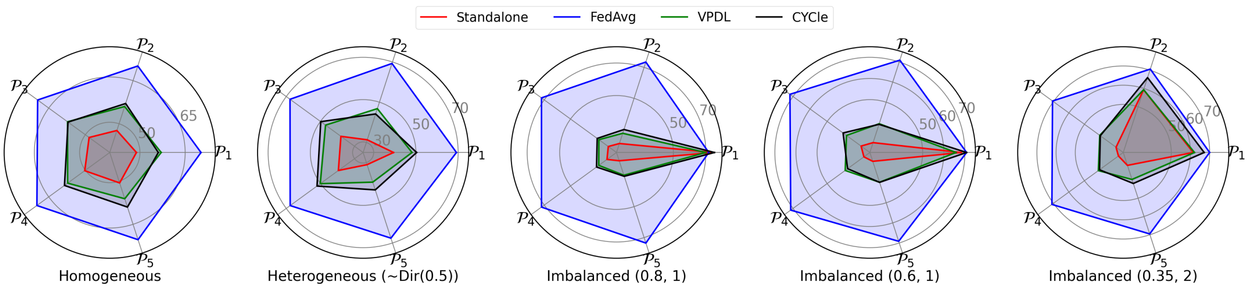

Figure 17: Per-participant performance comparison on CIFAR-100 dataset: Validation accuracy evaluated with $N = 5$ participants.

Table 7: Performance comparison on CIFAR-100 dataset: Validation accuracy evaluated with $N = 5$ participants. The table presents the performance of our proposed framework compared to the FedAvg algorithm. We employ MVA (↑), MCG (↑) and CGS (↓) as evaluation metrics.

Setting	**Homogeneous**			**Dirichlet (0.5)**			**Imbalanced (0.8, 1)**			**Imbalanced (0.35, 2)**			**Imbalanced (0.6, 1)**		
Metric	**MVA**	**MCG**	**CGS**	**MVA**	**MCG**	**CGS**	**MVA**	**MCG**	**CGS**	**MVA**	**MCG**	**CGS**	**MVA**	**MCG**	**CGS**
FedAvg	70.02	20.86	1.07	68.31	32.46	3.98	72.60	40.77	21.77	70.33	28.22	15.06	70.80	33.56	15.54
VPDL	56.74	7.58	1.20	46.36	10.51	2.59	36.81	4.98	4.84	48.48	6.37	5.19	44.61	7.37	4.98
CYCle	57.56	8.40	**0.69**	47.98	12.13	**0.68**	39.09	7.26	**3.30**	51.03	8.92	**2.40**	45.68	8.44	**3.00**

the FedAvg algorithm results in a decline in accuracy for $\mathcal{P}_1$, indicative of a negative collaboration gain. Following this, we compile the mean validation accuracy (MVA), mean collaboration gain (MCG), and collaboration gain spread (CGS) for each method and data splitting scenario in Table 7.

D.5 Imbalanced Data Study

In this study, we explore a range of values for the parameters κ and m in imbalanced settings, as detailed in Section 5.1. The purpose of this variation is to demonstrate the effectiveness of our proposed CYCle method in ensuring positive collaboration gains for each participant, showcasing a higher degree of fairness in comparison to FedAvg and VPDL. For a comprehensive view of these results, please see Figure 18 and Table 8.

Table 8: Performance comparison on CIFAR-10 dataset under imbalanced data: Validation accuracy evaluated with $N = 5$ participants. We employ MVA (↑), MCG (↑) and CGS (↓) as evaluation metrics.

Setting	**Imbalanced (0.4, 1)**			**Imbalanced (0.12, 1)**			**Imbalanced (0.41, 2)**			**Imbalanced (0.23, 2)**			**Imbalanced (0.14, 2)**		
Metric	**MVA**	**MCG**	**CGS**	**MVA**	**MCG**	**CGS**	**MVA**	**MCG**	**CGS**	**MVA**	**MCG**	**CGS**	**MVA**	**MCG**	**CGS**
FedAvg	91.04	10.38	4.93	90.98	8.02	4.00	90.17	17.48	13.99	91.23	7.73	1.96	90.89	8.42	4.94
VPDL	83.36	2.69	3.04	86.18	3.22	2.74	74.90	2.22	4.17	85.82	2.33	2.09	86.18	3.70	3.67
CYCle	85.02	4.35	**2.26**	86.78	3.82	**2.41**	76.71	4.02	**2.27**	86.48	2.98	**1.17**	86.92	4.44	**3.47**

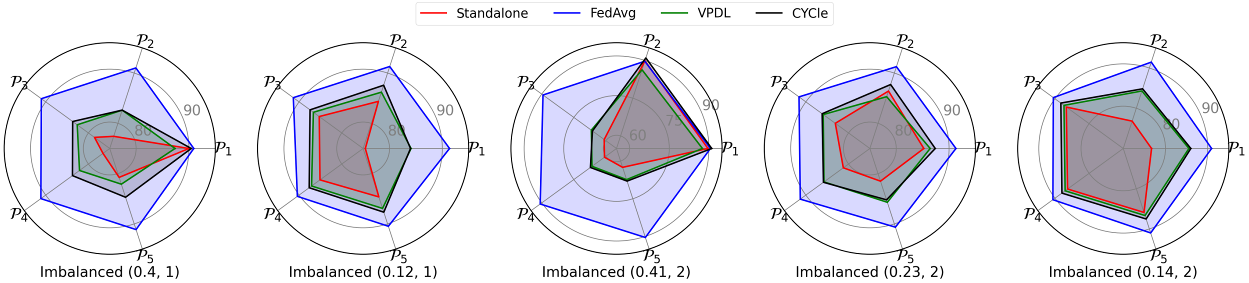

Imbalanced (0.4, 1)   Imbalanced (0.12, 1)   Imbalanced (0.41, 2)   Imbalanced (0.23, 2)   Imbalanced (0.14, 2)

Figure 18: Per-participant performance comparison on CIFAR-10 dataset using the given imbalanced splitting scenarios.

D.6 Free Rider Study

In Table 9 and Figure 19, we examine the outcomes using our CYCle approach under the varying degrees of label flipping (ranging from 0.0 to 1.0) when two participants ($\mathcal{P}_4$ and $\mathcal{P}_5$) are free riders. The findings show that the honest participants ($\mathcal{P}_1$, $\mathcal{P}_2$, and $\mathcal{P}_3$) maintain positive collaboration gains, despite the presence of malicious users / free riders. It's observed that when the flip rate is greater than 0, the collaboration gain decreases relative to scenarios where the flip rate is 0. This decline is linked to the fact that these three participants collectively hold only 60% of the total dataset. In this experiment, we use CIFAR-10 dataset and a homogeneous data splitting approach, with other parameters remaining consistent with those detailed in Section 5.1.

Table 9: Validation accuracies of participants ($\mathcal{P}_1 - \mathcal{P}_5$) with $\mathcal{P}_4$ and $\mathcal{P}_5$ having varying rates of label flipping. The last column refers to the average accuracy of honest participants ($\mathcal{P}_1 - \mathcal{P}_3$).

Setting	$\mathcal{P}_1$	$\mathcal{P}_2$	$\mathcal{P}_3$	$\mathcal{P}_4$	$\mathcal{P}_5$	avg
Standalone ($\mathcal{B}_n$)	83.42	83.67	83.15	83.13	83.63	83.41
Flip rate = 0.0	86.12	87.03	86.33	85.62	86.10	86.49
Flip rate = 0.2	84.25	84.20	84.10	63.10	65.40	84.18
Flip rate = 0.5	84.30	84.00	83.95	38.95	35.75	84.08
Flip rate = 1.0	84.15	84.20	83.45	3.40	3.10	83.93

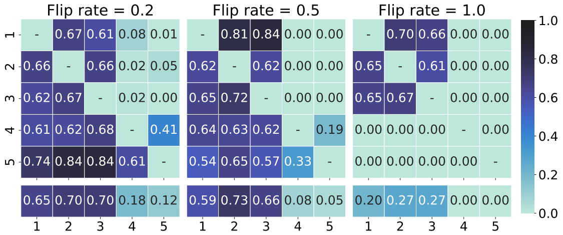

Figure 19: Heatmap visualization of reputation scores with corrupted labels at $\mathcal{P}_4$ and $\mathcal{P}_5$.

D.7 Hyperparameter Sensitivity

CYCle (PDL). We have defined only two hyperparameters in our model, τ_{opt} and τ_{max}, which have a geometric interpretation (degree of gradient alignment required for beneficial collaboration). In our experiments, we set $\tau_{opt} = 0.25$ and $\tau_{max} = 0.75$. Figure 20a shows the sensitivity analysis for these hyperparameters, where it is evident that increasing the values of τ_{max} and τ_{opt} correlates with improved MCG in a homogeneous setting. This is expected as higher values of these parameters bring our algorithm closer to the VPDL framework. However, the MCG and CGS (Figure 20b) values for different hyperparameter settings are comparable, indicating that the reported results are robust.

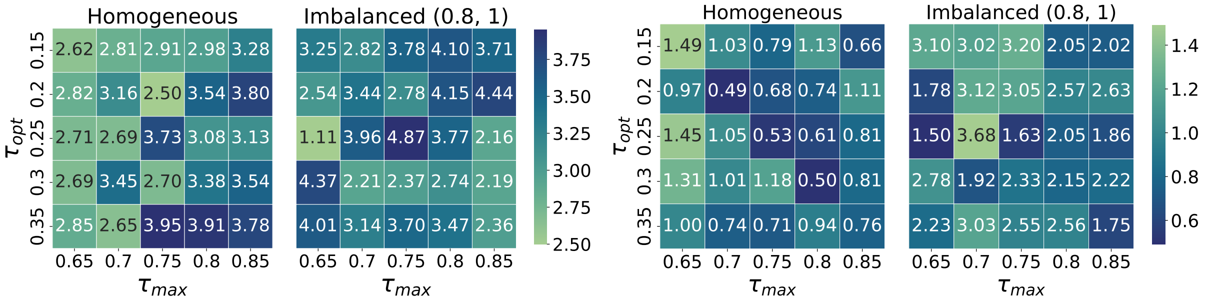

(a) MCG (↑)

(b) CGS (↓)

Figure 20: Sensitivity analysis to τ_{opt} and τ_{max} parameters.

CYCle (Gossip-SGD). The only hyperparameter in the gossip-based variant of our protocol is β, which controls the sharpness of the softmax function used to derive the communication probabilities from gradient alignment scores. Higher β values assign greater weight to stronger alignments, enforcing more selective and fairness-oriented peer interactions, while lower values yield more uniform communication,

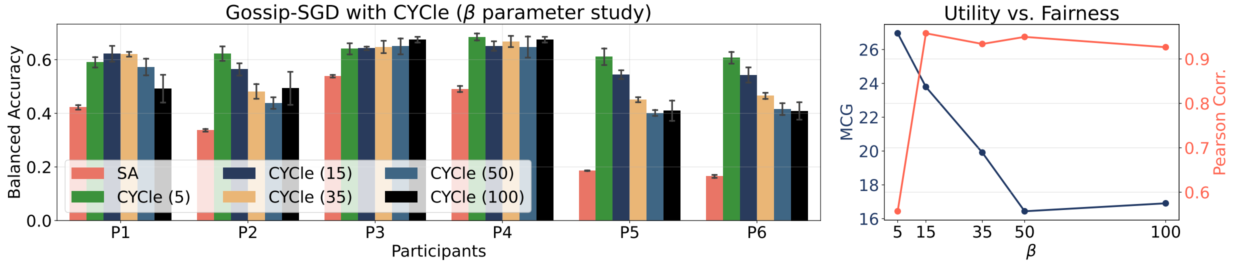

(a) Performance of CYCle under different β parameters $\in \{5, 15, 35, 50, 100\}$. (b) MCG vs. correlation coefficient.

Figure 21: Study on the impact of parameter β on performance and analysis of the utility versus fairness trade-off using the CYCle algorithm.

resembling a fully connected topology. Figure 21a shows the performance across participants under varying $\beta \in \{5, 15, 35, 50, 100\}$. Although participant-level performance varies slightly, all configurations exhibit reasonable fairness, validating the robustness of CYCle under different settings. Figure 21b further illustrates the trade-off between utility (MCG) and fairness (Pearson correlation of pre- and post-collaboration accuracies). We observe that intermediate values of β (e.g., 35-50) strike a favorable balance, delivering high collaboration gain without sacrificing fairness.

D.8 Additional Results

The accuracy metrics for the individual participants for the experiments on CIFAR-10 dataset (corresponding to Figures 3 and 4) are summarized in Table 10 for greater clarity. These results clearly demonstrate the negative gain experienced by participant $\mathcal{P}_1$ in the imbalanced settings under most existing FL algorithms and how the proposed CYCle approach overcomes this problem.

Table 10: Per-participant performance comparison on CIFAR-10 dataset: Validation accuracy evaluated with $N = 5$ participants. The left table presents the performance of our proposed framework compared to the FedAvg algorithm. The right table compares collaboration gain and fairness of our proposed CYCle algorithm with existing works (columns 4-6). We employ MVA (↑), MCG (↑) and CGS (↓) as evaluation metrics.

Split	**No./Metric**	**SA**	**FedAvg**	**VPDL**	**CYCle**
Homogeneous	1	83.42	91.02	85.82	86.12
	2	83.67	90.32	84.02	87.03
	3	83.15	90.63	84.70	86.33
	4	83.13	90.82	85.27	85.62
	5	83.63	90.23	85.12	86.10
	MVA	83.40	90.60	84.98	86.24
	MCG	0.00	**7.20**	1.58	2.84
	CGS	0.00	0.48	0.71	**0.37**
Dirichlet (0.5)	1	68.47	88.92	74.47	79.48
	2	65.25	88.48	74.17	73.55
	3	73.92	88.35	77.17	79.87
	4	67.55	88.68	74.17	78.70
	5	61.62	89.35	71.40	73.05
	MVA	67.36	88.76	74.27	76.93
	MCG	0.00	**21.40**	6.91	9.57
	CGS	0.00	4.31	2.31	**2.13**
Imbalanced (0.8, 1)	1	92.77	90.23	89.87	93.80
	2	56.85	90.33	60.77	63.02
	3	53.82	90.07	62.08	62.82
	4	58.00	90.15	61.52	63.35
	5	57.68	90.07	61.68	63.30
	MVA	63.82	90.17	67.18	69.26
	MCG	0.00	**26.35**	3.36	5.44
	CGS	0.00	14.51	3.58	**2.56**
Imbalanced (0.35, 2)	1	89.30	90.45	85.50	89.90
	2	88.98	90.53	86.00	89.73
	3	69.07	89.83	73.97	75.35
	4	69.23	90.40	74.53	75.58
	5	69.53	90.48	73.55	75.02
	MVA	77.22	90.34	78.71	81.12
	MCG	0.00	**13.12**	1.49	3.89
	CGS	0.00	9.61	4.01	**2.65**
Imbalanced (0.6, 1)	1	92.27	90.38	89.25	92.80
	2	68.65	90.73	71.58	71.80
	3	69.12	89.92	71.53	72.65
	4	68.78	89.33	72.85	73.45
	5	70.60	90.43	71.95	72.87
	MVA	73.88	90.16	75.43	76.72
	MCG	0.00	**16.28**	1.55	2.83
	CGS	0.00	9.11	2.45	**1.38**

Split	**No./Metric**	**SA**	**CFFL**	**RFFL**	**CGSV**	**CYCle**
Homogeneous	1	60.98	62.05	61.65	63.32	72.42
	2	59.87	63.60	62.32	63.67	70.88
	3	59.20	61.58	61.07	63.08	71.48
	4	60.50	62.50	60.80	61.88	72.55
	5	61.67	63.53	61.65	64.42	72.43
	MVA	60.44	62.65	61.50	63.27	71.95
	MCG	0.00	2.21	1.05	2.83	**11.51**
	CGS	0.00	0.87	0.95	0.94	**0.58**
Dirichlet (0.5)	1	48.17	47.65	48.45	55.30	51.78
	2	48.72	49.28	50.07	53.10	53.20
	3	49.15	51.15	50.70	53.60	53.82
	4	44.17	49.30	45.72	54.70	47.95
	5	42.57	47.82	47.65	55.57	49.28
	MVA	46.55	49.04	48.52	54.45	51.21
	MCG	0.00	2.49	1.96	**7.90**	4.65
	CGS	0.00	2.35	1.63	3.40	**1.11**
Imbalanced (0.8, 1)	1	74.32	69.38	71.47	56.55	77.15
	2	52.95	56.08	52.80	56.92	57.10
	3	48.95	55.52	52.13	54.77	58.73
	4	48.40	54.97	52.40	55.33	57.93
	5	51.30	57.35	52.53	56.23	58.08
	MVA	55.18	58.66	56.27	55.96	61.80
	MCG	0.00	3.48	1.08	0.78	**6.62**
	CGS	0.00	4.39	**2.45**	9.32	**2.79**
Imbalanced (0.35, 2)	1	69.43	66.38	64.22	63.10	74.13
	2	69.70	68.52	63.55	62.15	74.07
	3	45.17	62.18	53.70	60.58	64.93
	4	44.02	63.93	54.12	61.53	63.93
	5	47.12	64.37	56.98	62.60	64.23
	MVA	55.09	65.08	58.51	61.99	68.26
	MCG	0.00	9.99	3.43	6.91	**13.17**
	CGS	0.00	9.95	7.46	11.34	**7.12**
Imbalanced (0.6, 1)	1	74.23	69.30	61.58	62.33	76.22
	2	45.08	65.70	49.05	61.43	64.17
	3	46.08	62.05	47.15	60.40	61.88
	4	43.80	63.97	48.67	60.53	59.10
	5	45.05	64.98	50.30	61.98	63.30
	MVA	50.85	65.20	51.35	61.34	64.93
	MCG	0.00	**14.35**	0.50	10.49	**14.08**
	CGS	0.00	9.79	6.74	11.23	**6.22**